Steroid Receptor Coactivator-1 Modulates the Function of Pomc Neurons and Energy Homeostasis

Yongjie Yang[1~], Agatha A. van der Klaauw[2~], Liangru Zhu[1,3~], Tessa M. Cacciottolo[2~], Yanlin He[1], Lukas K.J. Stadler[2], Chunmei Wang[1], Pingwen Xu[1], Kenji Saito[1], Antentor Hinton Jr.[1], Xiaofeng Yan[1], Julia M. Keogh[2], Elana Henning[2], Matthew C. Banton[2], Audrey E. Hendricks[4,5], Elena G. Bochukova[2], Vanisha Mistry[2], Katherine L. Lawler[2], Lan Liao[6], Jianming Xu[6], Stephen O'Rahilly[2], Qingchun Tong[7], UK10K consortium, Inês Barroso[4], Bert W. O'Malley[6], I. Sadaf Farooqi[2*], Yong Xu[1, 6*]

[1]Children's Nutrition Research Center, Department of Pediatrics, Baylor College of Medicine, One Baylor Plaza, Houston, TX 77030, USA; [2]University of Cambridge Metabolic Research Laboratories and NIHR Cambridge Biomedical Research Centre, Wellcome Trust-MRC Institute of Metabolic Science, Addenbrooke's Hospital, Cambridge, CB2 0QQ, UK; [3]Division of Gastroenterology, Union Hospital, Tongji Medical College, Huazhong University of Sciences & Technology, China; [4]Wellcome Sanger Institute, Cambridge, UK; [5]Mathematical and Statistical Sciences Department, University of Colorado – Denver, Denver, CO 80204, USA; [6]Department of Molecular and Cellular Biology, Baylor College of Medicine, Houston, TX 77030, USA; [7]Brown Foundation Institute of Molecular Medicine, University of Texas Health Science Center at Houston, Houston, TX 77030, USA.

[~,*] These authors contributed equally to this work. To whom correspondence should be addressed: Y. X. E-mail: yongx@bcm.edu Ph: 1-713-798-7199 Fax: 1-713-798-7187 and I.S.F. E-mail: isf20@cam.ac.uk Ph: 44-1223-762634 Fax: 44-1223-762657.

Abstract

Hypothalamic neurons expressing the anorectic peptide Pro-opiomelanocortin (Pomc) regulate food intake and body weight. Here, we show that Steroid Receptor Coactivator-1 (SRC-1) interacts with a target of leptin receptor activation, phosphorylated STAT3, to potentiate Pomc transcription. Deletion of *SRC-1* in Pomc neurons in mice attenuates their depolarization by leptin, decreases *Pomc* expression and increases food intake leading to high-fat diet-induced obesity. In humans, fifteen rare heterozygous variants in *SRC-1* found in severely obese individuals impairs leptin-mediated Pomc reporter activity in cells, whilst four variants found in non-obese controls do not. In a knock-in mouse model of a loss of function human variant (SRC-1^{L1376P}), leptin-induced depolarization of Pomc neurons and *Pomc* expression are significantly reduced, and food intake and body weight are increased. In summary, we demonstrate that SRC-1 modulates the function of hypothalamic Pomc neurons, and suggest that targeting SRC-1 may represent a useful therapeutic strategy for weight loss.

Introduction

Transcriptional coactivators and corepressors regulate the ability of nuclear hormone receptors (NRs) and transcription factors (TFs) to enhance/suppress the expression of target genes by facilitating the assembly of the transcription complex at target gene promoters[1]. Understanding the molecular mechanisms by which coactivators and corepressors alter gene expression to modulate physiological processes may provide insights into disease mechanisms and highlight potential therapeutic targets.

Steroid receptor coactivator (SRC)-1 belongs to a family of coactivators (SRC-1, -2 and -3) that mediate NR-dependent or TF-dependent transcription[2]. Global deletion of SRC-1 in mice leads to obesity[3]; however, to date, the molecular mechanisms involved are incompletely understood. SRC-1 is abundantly expressed in the hypothalamus, including neurons within the arcuate nucleus of the hypothalamus (ARH)[4], which play a key role in mediating the weight-reducing effects of the adipocyte-derived hormone leptin[5, 6]. Leptin is a signal of nutrient deprivation, with a fall in leptin levels triggering a set of responses that seek to restore energy homeostasis by increasing food intake and decreasing energy expenditure[7]. In the fed state, an increase in leptin levels leads to the activation of neurons expressing the anorectic peptide Pro-opiomelanocortin (POMC) leading to a reduction in food intake[8]. Specifically, leptin binding to its receptor phosphorylates the transcription factor STAT3 which dimerises and translocates to the nucleus where it stimulates the expression of POMC[9, 10, 11]. Leptin-induced STAT3 activation also stimulates expression of *Socs3* (suppressor of cytokine signaling-3) which acts to inhibits leptin signaling[12, 13].

In this study, we sought to investigate the central mechanisms by which SRC-1 modulates

energy homeostasis. SRC family members bind to STAT transcription factors in cells[14]. Thus, we first examined the effects of SRC-1 on STAT3 transcriptional activity and Pomc expression. We then characterized metabolic phenotypes in mice lacking SRC-1 in Pomc neurons and explored the underlying mechanisms. Additionally, we examined the potential functional consequences of rare human variants in *SRC-1* identified in severe childhood-onset obesity. Finally, we generated a knock-in mouse model of the most severe loss of function human SRC-1 variant and characterized the metabolic consequences of these mutant mice.

Results

SRC-1 interacts with pSTAT3 to stimulate Pomc expression

We found that global *SRC-1-KO* mice [15] had lower *Pomc* but normal *Socs3* mRNA levels in the hypothalamus compared to control littermates (Figure 1a). Using Chromatin-immunoprecipitation (ChIP) assays, we found that leptin-stimulated pSTAT3 binding to *Pomc* promoters was decreased in the hypothalamus of *SRC-1-KO* mice compared to control mice (Figure 1b). In keeping with these findings, *SRC-1* overexpression potentiated STAT3-induced *Pomc* transcription but had no effect on *Socs3* transcription in Neuro2A cells and HEK293 cells (Figure 1C-D; Supplementary Figure 1a-b). Similar effects of *SRC-1* were observed in *SRC-1-KO* MEFs cells, although STAT3 alone could stimulate *Pomc* expression in these cells devoid of endogenous SRC-1 (Supplementary Figure 1c-d). These results indicate that SRC-1, while not required for STAT3 transcriptional activity, can facilitate STAT3-induced *Pomc* expression.

SRC-1 in Pomc neurons regulates energy homeostasis

To test whether SRC-1 in Pomc neurons plays a functionally significant role in energy homeostasis, we crossed *SRC-1*$^{lox/lox}$ mice with *Pomc-Cre* mice to generate mice lacking *SRC-1* selectively in *Pomc* lineage cells (pomcSRC-1-KO, Supplementary Figure 1e). On a standard chow diet, the body weight of male pomcSRC-1-KO mice was comparable to control littermates (*SRC-1*$^{lox/lox}$) (Supplementary Figure 1f), whilst female pomcSRC-1-KO mice showed significant weight gain (Supplementary Figure 1g). This sexual dimorphism may be explained by our earlier observations that global *SRC-1* deficiency blunts the weight-reducing effects of estrogen[4]. On a high fat diet (HFD), male pomcSRC-1-KO mice gained significantly more weight compared to control littermates (Figure 1e) due to an increase in fat mass (Figure 1f). In weight-matched mice, we observed a significant increase in HFD intake in pomcSRC-1-

KO mice vs controls (Figure 1g-h); measurements of energy expenditure were comparable (Supplementary Figure 1h-j).

A caveat of the regular *Pomc-Cre* mouse line is that, during the early development, Cre recombinase is transiently expressed in a broader population of neurons and some of these *Pomc* lineage cells mature into orexigenic Npy/Agrp neurons with opposing effects on food intake[16]. To address this concern, we crossed a *Pomc-CreER* transgene[17] onto the *SRC-1$^{lox/lox}$* mouse allele. Tamoxifen induction at 9 weeks of age resulted in deletion of SRC-1 in mature *Pomc* neurons (MpomcSRC-1-KO; Supplementary Figure 1k-l). When fed with a HFD, MpomcSRC-1-KO mice displayed increased weight gain and fat mass, associated with increased food intake compared to control littermates (Figure 1i-k), which recapitulated the phenotypes observed in *pomcSRC-1-KO* mice. Collectively, these results indicate that SRC-1 in mature *Pomc* neurons is required to defend against diet-induced obesity.

SRC-1 in Pomc neurons is required for the anorectic effects of leptin

Several studies have shown that STAT3 signaling is a mediator of leptin's effects on body weight[10, 18]. In HFD-fed *pomcSRC-1-KO* mice, we observed a 5-6-fold increase in circulating leptin levels in HFD-fed *pomcSRC-1-KO* mice (Figure 2a), whilst adiposity only increased 2-fold (Figure 1f). Thus, we hypothesized that SRC-1 is downstream of leptin action and loss of SRC-1 in *Pomc* neurons may impair leptin signaling. Supporting this possibility, we found that intra-peritoneal administration of leptin to control mice rapidly increased the hypothalamic SRC-1-pSTAT3 interaction (Figure 2b-c). Leptin administration significantly reduced 1-hour food intake in control mice but not in pomcSRC-1-KO mice (Figure 2d), despite increased leptin-induced pSTAT3 in the arcuate nucleus (Figure 2e-f). These results suggest that the SRC-1-

pSTAT3 interaction is downstream of leptin-STAT3 signaling, and contributes to the acute anorectic effects of leptin. Notably, the effects of leptin on 4-hour and 24-hour food intake were not significantly altered in pomcSRC-1-KO mice (Supplementary Figure 2a-b), presumably because the anorectic effects of leptin after the first hour are mediated by other leptin-responsive neurons or other signaling pathways[19, 20].

~~Since~~ L~~l~~eptin also depolarizes a subset of Pomc neurons to exert its anorectic effects[8], although recent fiber photometry studies failed to detect acute effects of leptin on calcium dynamics in Pomc neurons[21]. Thus, we examined leptin-induced depolarization in TOMATO-labelled mature Pomc neurons from *MpomcSRC-1-KO* mice and tamoxifen-treated controls after one-week HFD feeding. We recorded leptin-induced changes in resting membrane potential (RM) in the presence of tetrodotoxin (TTX), which blocks action potentials, and a mixture of fast synaptic inhibitors which block the majority of presynaptic inputs. We found that 26/39 (67%) of Pomc neurons from control mice were depolarized (>2 mV elevations in RM) by leptin (Figure 2g-h). In contrast, only 14/43 (33%) of Pomc neurons from *MpomcSRC-1-KO* mice were depolarized by leptin (P=0.002) and the amplitude of leptin-induced depolarization was significantly reduced in these Pomc neurons (Figure 2g-i). Interestingly, in the absence of TTX and synaptic inhibitors, leptin-induced depolarization and increases in firing frequency were comparable between the two groups (Supplementary Figure 2c-f), suggesting that indirect effects of leptin through presynaptic terminals[22, 23] were not affected by loss of SRC-1 in Pomc neurons. Notably, the baseline firing frequency was significantly decreased in mature Pomc neurons from MpomcSRC-1-KO mice compared to those from control mice, whereas the baseline RM remained unchanged (Figure 2j-l). We found that the amplitude, but not the frequency, of miniature inhibitory postsynaptic currents (mIPSC) was

145 significantly higher in mature Pomc neurons from MpomcSRC-1-KO mice than those from
146 control mice (Figure 2m-o). The frequency of mIPSC is thought to reflect presynaptic events
147 (e.g. GABA release), while mIPSC amplitude is largely determined by responsiveness of
148 postsynaptic neurons. Thus we suggest that SRC-1 also regulates the responsiveness of Pomc
149 neurons to GABA-ergic inputs via a leptin-independent mechanism.
150
151 **Rare SRC-1 variants found in obese humans impairs SRC-1 functions**
152 We next investigated the potential role of SRC-1 in humans by interrogating exome
153 sequencing and targeted resequencing data on 2,548 European ancestry individuals with
154 severe, early-onset obesity (mean body mass index [BMI] standard deviation score = 3; age of
155 onset <10 years) and 1,117 ancestry-matched controls[24]. Eleven rare heterozygous variants
156 in *SRC-1* were identified; another 8 variants were identified in an earlier data release (total
157 n=19). Fifteen *SRC-1* variants were identified only in obese cases (N1212K was found in two
158 unrelated obese individuals); the other 4 variants were found in controls (Figure 3a).
159 Compared to WT SRC-1, six of seven randomly selected SRC-1 mutants found in obese cases
160 (except for S738L) were significantly impaired in their interaction with pSTAT3 in leptin-
161 treated HEK293 cells (Figure 3b-c, Supplementary Figure 3a-c). To test whether heterozygous
162 *SRC-1* variants exerted a dominant negative effect to inhibit the interaction between WT SRC-
163 1 and pSTAT3, we overexpressed SRC-1 mutants in HEK293 cells which endogenously express
164 SRC-1. After leptin treatment, an anti-pSTAT3 antibody was used to pull down the
165 immunocomplex from cell lysates, followed by immunoblotting with an anti-SRC-1 antibody
166 to examine the interaction between pSTAT3 and total SRC-1. Overexpression of SRC-1
167 mutants found in obese cases (6 of 7 tested mutants) significantly decreased the interaction
168 between pSTAT3 and the total SRC-1, suggesting that these SRC-1 mutants can impair the

ability of WT SRC-1 to interact with pSTAT3 (Figure 3d-e and Supplementary Figure 3d-e). This dominant negative effect was not seen when testing the 4 mutants found in controls (Figure 3e and Supplementary Figure 3d). We used a POMC-luciferase reporter assay to examine the effects of leptin on *Pomc* expression. We found that WT SRC-1 significantly enhanced leptin-induced Pomc-luciferase reporter activity, but co-expression of a dominant negative form of STAT3 abolished this effect (Supplementary Figure 3f-g), suggesting that the interaction with STAT3 is required for the observed effects of SRC-1 on *Pomc* transcription. Fourteen of fifteen SRC-1 mutants found in severely obese cases (except for S738L) significantly impaired leptin-induced *Pomc* expression, whereas the 4 control mutants exhibited WT-like responses in this assay (Figure 3f). Interactions with estrogen receptor-α, vitamin D receptor, glucocorticoid receptor, thyroid hormone receptor-β, and peroxisome proliferator-activated receptor γ (PPARγ) were comparable to those seen for WT SRC-1 (Supplementary Figure 4) in co-immunoprecipitation assays.

A mouse model of the human SRC-1 variant L1376P is obese

To directly test whether rare human SRC-1 variants contribute to Pomc neuron function and/or energy homeostasis, we generated a knock-in mouse model of a human variant which results in a severe loss of function in cells, SRC-1^{L1376P} (Figure 4a). Heterozygous mutant mice (SRC-$1^{L1376P/+}$) fed a HFD exhibited increased weight gain, adiposity and food intake, associated with reduced Pomc mRNA levels compared to WT controls (Figure 4b-e). We recorded leptin-induced depolarization in Pomc neurons in control vs *SRC-1*$^{L1376P/+}$ mice one week after HFD feeding. In control mice, 13/19 (68%) Pomc neurons were depolarized by leptin, whilst only 5/18 (26%) Pomc neurons from SRC-$1^{L1376P/+}$ mice were depolarized by leptin (P=0.022) and the amplitude of leptin-induced depolarization was significantly reduced

193 in these Pomc neurons (Figure 4f-h). Baseline firing frequency and resting membrane
194 potential were both significantly decreased in Pomc neurons from SRC-1$^{L1376P/+}$ mice
195 compared to those from control mice (Figure 4i-k). Further, the amplitude, but not the
196 frequency, of the mIPSC was significantly higher in Pomc neurons from SRC-1$^{L1376P/+}$ mice than
197 those from control mice (Figure 4l-n). Thus, these data indicate that the SRC-1^{L1376P} variant
198 causes obesity in mice, associated with decreased Pomc expression and decreased Pomc
199 neuron excitability through both leptin-dependent and independent mechanisms.
200

Discussion

In this study, we demonstrated that in the hypothalamus, the coactivator SRC-1 modulates the ability of leptin to regulate the expression of the anorectic peptide POMC by directly interacting with phosphorylated STAT3, a known product of leptin-receptor activation. In mice, disruption of SRC-1 in Pomc neurons led to increased food intake, weight gain on a HFD and impaired the acute anorectic response to leptin administration demonstrating the physiological relevance of this molecular interaction. The modest degree of obesity in these mice was comparable to that seen with inactivation of STAT3 in Pomc neurons[9] and studies demonstrating that direct leptin action on Pomc neurons accounts for a proportion of leptin's effects on body weight[20, 25, 26, 27]. The obesity seen in SRC-1 deletion or mutant mice was less severe than that see in mice deficient in Pomc [28] or melanocortin 4 receptor [29] in keeping with SRC-1's role as a modulator of Pomc expression. Additionally, leptin-responsive Agrp neurons have been shown to play a major role in energy homeostasis[20].

We identified 15 rare heterozygous variants in *SRC-1* in 16 severely obese individuals and 4 rare variants in controls. Notably, there are several low frequency and many rare variants in this gene in publically available databases (http://gnomad.broadinstitute.org/). Some of these low frequency variants have been shown to have functional consequences, for example, P1272S (MAF: 3.16% in cases, 3.45% in controls; 1.66% in gnomAD) disrupts a putative glycogen synthase 3 (GSK3)β phosphorylation site and has been shown to exhibit reduced ability to co-activate Estrogen Receptor in multiple cell lines[30]. Genetic studies in larger numbers of cases and controls with functional studies of all variants identified will be needed to establish whether variants that result in a loss of function when tested in cells are more

likely to be found in severely obese individuals than in controls. In this study, the variants found in obese individuals, but not those found in controls, were associated with impaired interaction with pSTAT3 and reduced POMC reporter activity in cells, predominantly through a dominant negative effect. Given the challenges associated with studying such rare variants, and to directly test whether rare human SRC-1 variants contribute to Pomc neuron function and/or energy homeostasis, we generated a knock-in mouse model of a human variant which results in a severe loss of function in cells, SRC-1^{L1376P}. The increased food intake and weight gain in heterozygous knock-in mice carrying a severe loss of function human SRC-1 variant supports the potential importance of the mechanism identified here in humans.

Recent evidence indicates that loss of leptin receptors in Pomc neurons does not affect body weight in chow-fed mice[20, 25]. In line with these reports, we show that loss of SRC-1 in Pomc neurons produced minor effects on energy balance in chow-fed male mice. These suggest that the physiological consequences of disrupting this interaction in normal weight animals are small and/or may be compensated for by increased signaling through non-POMC expressing leptin-responsive neurons[31] and/or signaling via phosphoinositide-3-kinase (PI3K)[32], mTOR/S6K[33] and/or AMPK pathways[34, 35]. We showed that SRC-1 deletion in Pomc neurons attenuated the acute anorectic response (1 hour) to leptin but not the late phase (4-24 hours). Cumulatively, these findings indicate that leptin-mediated POMC expression (modulated by the SRC-1-pSTAT3 interaction) primarily contributes to the acute anorectic response to leptin. In keeping with this finding, we demonstrated that the hypothalamic SRC-1-pSTAT3 interaction was enhanced by leptin. Consumption of HFD leads to sustained positive energy balance and an increase in leptin levels. The resulting increase in pSTAT3 would be

247 expected to stimulate POMC expression and reduce food intake, a response that we have
248 shown is modulated by the interaction between pSTAT3 and SRC-1. We suggest that in the
249 absence of functional SRC-1, pSTAT3 is less effective at stimulating POMC expression, which
250 manifests as a relative increase in food intake and weight gain when mice are challenged with
251 HFD. In this way, we conclude that SRC-1 acts as a positive regulator of leptin sensitivity in
252 hypothalamic Pomc neurons.

253

254 Our findings suggest that SRC-1 facilitates but is not required for pSTAT3 to regulate *Pomc*
255 expression and that this effect is target-specific as SRC-1 does not modulate the ability of
256 pSTAT3 to regulate *Socs3*. The mechanisms underlying such specificity remain unclear at
257 present. The molecular interaction between SRC-1 and pSTAT3 enhances pSTAT3-mediated
258 transcriptional activity, presumably by stabilizing pSTAT3 binding to the POMC promoter,
259 although we cannot exclude the possibility that recruitment of other co-coactivators or
260 histone acetyltransferase activity of SRC-1 also may be involved[36]. Further studies of the
261 molecular mechanisms that modulate leptin signaling are emerging[37, 38, 39, 40, 41, 42]. For
262 example, Chen et al showed that the nuclear receptor Nur77 facilitates STAT3 acetylation by
263 recruiting acetylase p300 and disassociating deacetylase histone deacetylase 1 (HDAC1) to
264 enhance the transcriptional activity of STAT3[43]. In findings that parallel our studies, they
265 showed that Nur77 deficiency reduced the expression of Pomc in the hypothalamus and
266 attenuated the response to leptin in mice fed on a HFD[43].

267

268 Transcriptional coactivators such as SRC-1 facilitate the signaling mediated by multiple NRs
269 and/or TFs factors[2]. Several NRs/TFs have been shown to affect energy homeostasis through

their actions in the brain[44], including FoxO1[45, 46, 47, 48], ERα[49, 50], PPARγ[51, 52] and THR[53] and thus could contribute to the body weight phenotype seen with SRC-1 disruption in mice and loss of function variants in humans. In addition to the central actions of SRC-1 on energy homeostasis, SRC-1 is expressed in brown adipose tissue, where it appears to compete with SRC-2 to interact with the PPARγ-PGC1α complex. Picard et al showed that *SRC-1-KO* mice had reduced rectal temperatures upon cold exposure and reduced oxygen consumption although they did not quantify food intake in this study[3]. Notably, we did not observe any changes in energy expenditure in mice lacking SRC-1 in Pomc neurons, consistent with the notion that SRC-1 in other tissues may also contribute to the regulation of energy expenditure[3]. Whilst we found that SRC-1 variants detected in obese patients did not affect the interactions with a number of NRs, these results do not exclude the potential impact of SRC-1 variants on the signaling of these NRs which need to be explored in more detail using tissue-specific conditional knockout mouse models**.**

Targeting specific coactivator-mediated interactions has emerged as a potential therapeutic strategy to enhance signaling in some tissues while inhibiting signaling in others[54, 55]. For example, Selective Estrogen Receptor Modulators (SERMs) are effective in modulating the growth of hormone-responsive tumours (e.g. Tamoxifen in breast cancer) by impacting on coactivator stability and activity[56]. As such, compounds that target the interaction between SRC-1 and STAT3 at specific sites may potentially be used to modulate (ie: enhance) leptin signaling. Could this approach be efficacious in the treatment of obesity? Studies in mice and humans have consistently demonstrated that leptin sensitivity is greatest in those with no/very low endogenous circulating leptin levels[57, 58]. Whether enhancing leptin sensitivity in

293 the context of common obesity, which is associated with elevated leptin levels, may be
294 clinically beneficial, is the subject of much debate[18, 59, 60, 61]. The finding that some compounds
295 (e.g. the amylin derivative pramlintide) can augment the effects of leptin[62, 63], suggests that it
296 may be possible to increase the sensitivity of some individuals to therapeutic leptin
297 administration and that this approach may lead to weight loss. These observations and our
298 findings on SRC-1 suggest that pharmacological approaches based on the modulation of leptin
299 sensitivity could represent a potential therapeutic strategy for the treatment of obesity-
300 associated metabolic disease.
301

METHODS

CONTACT FOR REAGENT AND RESOURCE SHARING

Further information and requests for resources and reagents should be directed to and will be fulfilled by Yong Xu (yongx@bcm.edu) and Sadaf Farooqi (isf20@cam.ac.uk).

EXPERIMENTAL MODEL AND SUBJECT DETAILS

Mice

We crossed regular *Pomc-Cre* transgenic mice[27] and *SRC-1*$^{lox/lox}$ mice[64]. This cross produced pomcSRC-1-KO mice (those that are homozygous for *SRC-1*$^{lox/lox}$ and also carry the *Pomc-Cre* transgene) and control mice (those that are homozygous for *SRC-1*$^{lox/lox}$ but do not carry the *Pomc-Cre* transgene). These littermates were used to characterize the metabolic profile.

In addition, we also crossed inducible *Pomc-CreER* mice[17] with *SRC-1*$^{lox/lox}$ mice to generate MpomcSRC-1-KO mice (those that are homozygous for *SRC-1*$^{lox/lox}$ and also carry the *Pomc-CreER* transgene) and control mice (those that are homozygous for *SRC-1*$^{lox/lox}$ but do not carry the *POMC-CreER* transgene). Both these mice received tamoxifen injecitons (0.2 mg/g, i.p., twice at 9 weeks of age). These littermates were used to characterize the metabolic profile. For electrophysiological recordings, we crossed the inducible *Pomc-CreER* and the *Rosa26-tdTOMATO* mouse alleles onto *SRC-1*$^{lox/lox}$ mice, to produce MpomcSRC-1-KO mice with mature Pomc neurons labelled by TOMATO; as controls, we crossed inducible *Pomc-CreER* mice and *Rosa26-tdTOMATO* mice to generate *Pomc-CreER/Rosa26-tdTOAMTO* mice. In parallel, we also crossed the *Npy-GFP* mouse allele[23] and the *Rosa26-tdTOMATO* allele onto

inducible *Pomc-CreER* mice. This cross produced *Pomc-CreER/Rosa26-tdTOAMTO/Npy-GFP* mice, which were subjected to histology validation for the inducible *Pomc-CreER* mice.

To generate the *SRC-1*$^{L1376P/+}$ knock-in mice, a single-guide RNA (sgRNA) sequence was selected overlap amino acid residue L1382 (equivalent to human L1376) in SRC-1 (sgRNA 5'-CATCTGCGTCTGTTTTGAGAagg chr12:4253665-4253687; GRCm38/mm10) using the CRISPR Design Tool (Ran et al. 2013). A DNA templates for in vitro transcription of the sgRNA was produced using overlapping oligonucleotides in a high-fidelity PCR reaction[65], and sgRNA was transcribed using the MEGAshortscript T7 kit (ThermoFisher, Waltham, MA). Cas9 mRNA was purchased from ThermoFisher. The donor DNA template to introduce the L1382P point mutation, as well as a silent mutation D1381D to introduce a novel restriction site for Sau3AI, was purchased as an Ultramer from IDT (Coralville, IA). The sequence of ssODN is as follows (complementary to non-target strand): 5' TGAAAATCTG CTCTTTTGTT TATCCTTAAT AGATGAATGA TCCAGCACTG AGACACACAG GCCTCTACTG CAACCAGCTC TCGTCCACTG ATCCCCTCAA AACAGACGCA GATGGAAACC AGGTCAGTAA GAAA, where the homology arms are in bold. The mutations introduced in the donor sequence disrupt base 20 of the sgRNA and the PAM site to prevent additional mutagenesis. The BCM Genetically Engineered Mouse (GEM) Core microinjected Cas9 mRNA (100 ng/µl), Ultramer ssDNA (100 ng/µL), and sgRNA (20 ng/µl) into the cytoplasm of 200 pronuclear stage C57Bl/6J embryos. Cytoplasmic injections were performed using a microinjection needle (1 mm outer and 0.75 mm inner) with a tip diameter of 0.25–0.5 µm, an Eppendorf Femto Jet 4i to set pressure and time to control injection volume (0.5–1 pl per embryo). Injections were performed under a 200–400× magnification with Hoffman modulation contrast for visualizations. Founder animals (F_0) were identified by PCR-based restriction digestion to detect the CRISPR generated point mutations

in SRC-1. PCR product was first amplified with the primer pairs: 5'-CCTCACTTGTGGCAATGTGA and 5'-TCGTGGCAGTTCTGTAGTCAC; and then amplified with 2nd pairs: 5'-CACTGAGACACACAGGCCTC and 5'- ATCGAATCTGCCAGCTCTGC. The 121 bp PCR products were then digested with Sau3AI. 70 and 51 bp products after digest could be detected only for the mutated SRC-1 PCR products. Three independent lines were sequenced for the further confirmation of the point mutation. One of these lines was crossed to C57Bl6j to produce cohorts comprised of *SRC-1*$^{L1376P/+}$ and wild-type control mice. In some breedings, the *Pomc-CreER/Rosa26-tdTOAMTO* alleles were introduced to allow specific labelling of Pomc neurons.

In parallel, we crossed heterozygous *SRC-1-KO* mice[66] to heterozygous *SRC-1-KO* mice to produce homozygous *SRC-1-KO* and wild-type littermates. All the breeders have been backcrossed to C57Bl6 background for more than 12 generations. In addition, some C57Bl6 mice were purchased from the mouse facility of Baylor College of Medicine.

Care of all animals and procedures were approved by the Institutional Animal Care and Use Committee (IACUC) of Baylor College of Medicine Animal Facility, and all experimental procedures in animals complied with all relevant ethical regulations. Mice were housed in a temperature-controlled environment in groups of two to five at 22˚C-24˚C using a 12 hr light/12 hr dark cycle. Some cohorts were singly housed to measure food intake. The mice were fed either standard chow (6.5% fat, #2920, Harlan-Teklad, Madison, WI), or a 60% high fat diet (HFD, 60% fat, #D12492, Research Diets). Water was provided ad libitum.

Studies in mice

Validation of genomic deletion of SRC-1 in Pomc cells

Control mice, pomcSRC-1-KO mice or MpomcSRC-1-KO mice (after tamoxifen inductions) were anesthetized with inhaled isoflurane, and sacrificed. Various tissues, as detailed in the figures, were collected. Genomic DNAs were extracted using the REDExtract-N-Amp Tissue PCR Kit (#XNATS; Sigma-Aldrich, St Louis, MO), followed by PCR amplification of the floxed or recombined alleles. We used primers: forward- CAGTAAGGAATAGCAGATGTC and reverse-TGGCATCTATAACCAAATGTGTA TCA to detect the wild-type allele (a 560 bp band) and the floxed SRC-1 allele (a 630 bp band); and combined the reverse primer (mentioned above) with another forward primer: GTCGTACCATCTATGCCTCCTATAT to detect the recombined SRC-1 allele (a 320 bp band).

Histology

To validate specificity of the inducible *Pomc-CreER* transgene, *Pomc-CreER/Rosa26-tdTOAMTO/Npy-GFP* mice received tamoxifen injecitons (0.2 mg/g, i.p., twice) at 9 weeks of age, and then were perfused one week later. Brain sections were cut at 25 μm (1:5 series) and subjected to direct visualization of GFP and TOMATO signals using a Leica DM5500 fluorescence microscope with OptiGrid structured illumination configuration.

To examine effects of leptin on STAT3 phosphorylation in vivo, control and pomcSRC-1-KO mice (5 or 6 per group) were fasted overnight and then received a single bolus injection of saline or leptin (0.5 mg/kg, i.p.). Ninety minutes after the bolus injections, mice were anesthetized with inhaled isofluorane, and quickly perfused with 10% formalin, and brain sections were cut at 25 μm. The brain sections were pretreated (1% H_2O_2, 1%NaOH, 0.3% glycine, 0.03% SDS), blocked (3% Goat-anti-rabbit serum for 1 hour), incubated with rabbit anti-pSTAT3 antibody (1:2000; #9145, Cell Signaling) on shaker at room temperature for 24

hours and then put in 4 °C for 48 hours, followed by biotinylated anti-rabbit secondary antibody (1:1,000; Vector) for 2 hours. Sections were then incubated in the avidin-biotin complex (1:500, ABC; Vector Elite Kit) and incubated in 0.04% 3, 3'-diaminobenzidine and 0.01% hydrogen peroxide. After dehydration through graded ethanol, the slides were then immersed in xylene and cover-slipped. Images were analyzed using a brightfield Leica microscope. The numbers of pSTAT3-positive neurons in the ARH were counted by blinded investigators. For each mouse, pSTAT3-positive neurons were counted in 3-5 consecutive brain sections containing ARH, and the average was treated as the data value for that mouse. Five or six mice were included in each group for statistical analyses.

Body weight study

pomcSRC-1-KO mice and their control littermates were weaned at week 4. These mice were group housed and maintained on the standard chow (6.5% fat, #2920, Harlan-Teklad). At the age of day 97, mice were switched to the HFD (60% fat, #D12492, Research Diets) for 6 weeks. Body weight was measured every 4 days since weaning. Body composition was determined using quantitative magnetic resonance (QMR) on 28 days after HFD feeding. On day 42 after HFD feeding, the mice were deeply anesthetized with inhaled isoflurane and sacrificed. Blood was collected and processed to measure serum leptin using the mouse leptin ELISA kit (#90030, Crystal Chem, Inc). Serum samples with hemolysis (one from each group) were excluded from leptin ELISA assay. The gonadal white adipose tissue, the inguinal white adipose tissue, and the interscapular brown adipose tissue were isolated and weighed.

Similarly, MpomcSRC-1-KO mice and their control littermates were weaned at week 4. These mice were singly housed and maintained on the standard chow (6.5% fat, #2920, Harlan-

Teklad). All mice received tamoxifen injecitons (0.2 mg/g, i.p., twice) at 9 weeks of age. At the age of day 84, mice were switched to the HFD (60% fat, #D12492, Research Diets) for 30 days. Body weight and food intake were measured every 4 days. Body composition was determined using quantitative magnetic resonance (QMR) on 30 days after HFD feeding.

Food intake and energy expenditure

To further characterize the food intake and energy expenditure of pomcSRC-1-KO mice, an independent male cohort (pomcSRC-1-KO mice and their control littermates) was weaned on the standard chow. At the age of 12 weeks, these mice were acclimated into the Comprehensive Laboratory Animal Monitoring System (CLAMS). Mice were housed individually at room temperature (22°C) under an alternating 12:12-h light-dark cycle. After adaptation for 3 days, mice were subjected to a 2-day-chow-2-day-HFD protocol. Chow was replaced by HFD before the onset of dark cycle on day 3. Note that, the body weight and body composition were measured before the mice entered the CLAMS metabolic cages, and no difference was observed in body weight, fat mass and lean mass.

Another male cohort (pomcSRC-1-KO mice and their control littermates) was weaned on the standard chow. At the age of 11 weeks, these mice were singly housed and at week 12, the chow diet was replaced by HFD. HFD intake was measured every 2 days for 10 days.

Leptin-induced anorexia

Male pomcSRC-1-KO mice and their control littermates (chow-fed) were briefly fasted for 2 hours prior to the onset of dark cycle. These mice received intraperitoneal injections of saline or leptin (5 mg/kg in saline in a volume of 0.01 ml/g body weight) at 15 min prior to the dark

cycle. The standard chow was provided at the onset of dark cycle. Food intake was measured 1, 4 and 24 hours after food provision. Each mouse was tested with saline and leptin, administered in a counterbalanced order, with 4-day interval between the treatments.

Electrophysiology

For electrophysiological studies, *Pomc-CreER/Rosa26-tdTOMATO* (control) mice and *Pomc-CreER/Rosa26-tdTOMATO/SRC-1$^{lox/lox}$* (MpomcSRC-1-KO) mice received tamoxifen inductions (0.2 mg/g, i.p., twice at 9 weeks of age) and fed on HFD for one week. *Pomc-CreER/Rosa26-tdTOMATO/SRC-1$^{L1376P/+}$* and their control littermates (*Pomc-CreER/Rosa26-tdTOMATO*) were also fed on HFD for one week followed by electrophysiology recording as described below. Briefly, at 9:00am-9:30 am, these mice were deeply anesthetized with isoflurane and transcardially perfused with a modified ice-cold artificial cerebral spinal fluid (aCSF, in mM: 10 NaCl, 25 $NaHCO_3$, 195 Sucrose, 5 Glucose, 2.5 KCl, 1.25 NaH_2PO_4, 2 Na pyruvate, 0.5 $CaCl_2$, 7 $MgCl_2$)[48]. The mice were then decapitated, and the entire brain was removed. Brains was quickly sectioned in ice-cold aCSF solution (in mM: 126 NaCl, 2.5 KCl, 1.2 $MgCl_2$, 2.4 $CaCl_2$, 1 NaH_2PO_4, 11.1 Glucose, and 21.4 $NaHCO_3$)[23] saturated with 95% O_2 and 5% CO_2. Coronal sections containing the ARH (250 μm) was cut with a Microm HM 650V vibratome (Thermo Scientific). Then the slices were recovered in the aCSF[23] at 34 ℃ for 1 hr.

Whole-cell patch clamp recordings were performed in the TOMATO-labelled mature Pomc neurons in the ARH visually identified by an upright microscope (Eclipse FN-1, Nikon) equipped with IR-DIC optics (Nikon 40x NIR). Signals were processed using Multiclamp 700B amplifier (Axon Instruments), sampled using Digidata 1440A and analyzed offline on a PC with pCLAMP 10.3 (Axon Instruments). The slices were bathed in oxygenated aCSF[23] (32°C–34°C)

469 at a flow rate of approximately 2 ml/min. Patch pipettes with resistances of 3-5 MΩ were
470 filled with solution containing 126 mM K gluconate, 10 mM NaCl, 10 mM EGTA, 1 mM $MgCl_2$,
471 2 mM Na-ATP and 0.1 mM Mg-GTP (adjusted to pH7.3 with KOH).
472
473 Current clamp was engaged to test neural firing frequency and resting membrane potential
474 (RM) at the baseline and after puff application of leptin (300 nM, 1 second). In some
475 experiments, the aCSF solution also contained 1 μM tetrodotoxin (TTX) and a cocktail of fast
476 synaptic inhibitors, namely bicuculline (50 μM; a GABA receptor antagonist), DAP-5 (30 μM;
477 an NMDA receptor antagonist) and CNQX (30 μM; an AMPA receptor antagonist) to block the
478 majority of presynaptic inputs. The values for RM and firing frequency were averaged within
479 2-min bin at the baseline or after leptin puff. The RM values were calculated by Clampfit 10.3
480 using the "analysis→statistic" function of the software. A neuron was considered depolarized
481 or hyperpolarized if a change in membrane potential was at least 2 mV in amplitude and this
482 response was observed after leptin application and stayed stable for at least 2 minute. For
483 the miniature inhibitory postsynaptic current (mIPSC) recordings, patch electrodes were filled
484 with a recording solution that contained (in mM): 153.3 CsCl, 1.0 MgCl2, 5.0 EGTA, and 10.0
485 HEPES, pH of 7.20 with CsOH. CsCl was included to block potassium currents. Mg-ATP (3mM)
486 was added to the intracellular solution before recording. Glutamate receptor-mediated
487 synaptic currents were blocked by 30 μM D-AP-5 and 30 μM CNQX in the external solution,
488 along with 1 μM tetrodotoxin in the external solution blocking action potentials. Neurons
489 were voltage-clamped at -70 mV during the recording.
490
491 At the end of recordings, lucifer yellow dye was included in the pipette solution to trace the
492 recorded neurons and the brain slices were fixed with 4% formalin overnight and mounted

493 onto slides. Cells were then visualized with the Leica DM5500 fluorescence microscope to
494 identify post hoc the anatomical location of the recorded neurons in the ARH.
495
496 ***Real-time PCR analyses***
497 Total RNA was isolated using TRIzol Reagent (Invitrogen) according to the manufacturer's
498 protocol and reverse transcription reactions were performed from 2 μg of total RNA using a
499 High-Capacity cDNA Reverse Transcription Kits (Invitrogen). cDNA samples were amplified on
500 an CFX384 Real-Time System (Bio-Rad) using SsoADV SYBR Green Supermix (Bio-Rad). Correct
501 melting temperatures for all products were verified after amplification. Results were
502 normalized against the expression of house-keeping gene-Cyclophilin. Primer sequences were
503 listed in Supplementary Table 1.
504
505 ***Immunoprecipitation (Co-IP) and immunoblotting***
506 The harvested hypothalami were lysed in lysis buffer (50 mM Tris-HCl, pH 8.0, 50 mM KCl,
507 20mM NaF, 1mM Na3VO4, 10mM sodium pyrophosphate, 5 mM EDTA, and 0.5% Nonidet P-
508 40) supplemented with protease inhibitors (1 mm phenylmethylsulfonyl fluoride, and 20
509 μg/ml each of leupeptin, aprotinin, and pepstatin). Lysates were cleared by centrifugation at
510 18,000 × *g* for 10 min and used for immunoprecipitation or directly for immunoblotting. Equal
511 amounts of tissue lysates were incubated with anti-Phospho-STAT3 (Tyr705) (D3A7) XP-
512 Sepharose beads (Cell Signaling) or with a rabbit monoclonal SRC-1 (128E7) antibody (Cell
513 Signaling) after preclearing for overnight and pulled down with Protein A/G agarose beads
514 (Santa Cruz), respectively. Beads were washed three times with lysis buffer, and proteins
515 were released from beads in SDS-sample buffer and analyzed by immunoblotting. For
516 immunoblotting, protein samples were loaded onto SDS-polyacrylamide gels and transferred

to a nitrocellulose membrane. The blot was probed with a rabbit monoclonal SRC-1 (128E7) antibody at 1:3000 (Cell Signaling), a rabbit monoclonal phospho-STAT3 (Tyr705) (D3A7) XP antibody at 1:2000 (Cell Signaling), or a monoclonal anti-β-Actin antibody (AC-15) at 1:10000 (Sigma). The secondary antibody was rabbit anti-mouse IgG or goat anti-rabbit IgG (Jackson ImmunoResearch), both at a 1:10,000 dilution, followed by development with the SuperSignal West Pico Chemiluminescent Substrate (Pierce).

Chromatin immunoprecipitation assay (ChIP)

Fresh isolated hypothalami were homogenized and cross-linked in 1% formaldehyde. Then, the cross-linked protein-DNA complexes were sonicated to a length between 200 bp and 500 bp. The total chromatin (1%) was saved as an 'input' for later quantification. Complexes were pre-cleared and incubated with the Pierce Protein A/G Magnetic Beads (Thermo Scientific) and antibodies against STAT3 (sc-482; Santa Cruz) overnight at 4°C. Subsequently, cross-linking was reversed by overnight incubation at 65°C. DNAs were purified by phenol/chloroform extraction, ethanol precipitation and the enriched promoter fragments were measured by qPCR (primer sequences provided in Supplementary Table 1). Relative STAT3 promoter occupancy was adjusted to the background content of the negative control, and the initial chromatin input. The assays were repeated independently 3 times.

Generation of SRC-1 constructs and expression plasmids

The long form of SRC-1 containing a C-terminal Flag MYC tag was purchased from Origene (RC224812). The short form of SRC-1 was generated using the Q5 site directed mutagenesis kit (NEB) using primers containing the sequence specific to the short form of SRC-1. The N-terminal HA tag was added using the Q5 site directed mutagenesis kit (NEB) using primers

containing the HA tag sequence. The short and long forms of SRC-1 was then cloned into the pCDNA3.1(+) vector using KpnI and XhoI restriction sites after PCR amplification of SRC-1 using primers flanking the Origene KpnI and XhoI sites. SRC-1 mutant constructs were generated using the Quickchange II XL site directed mutagenesis kit (Agilent).

In vitro protein interaction

HEK293 (Human embryonic kidney 293) cells were transfected with either Flag tagged transcriptional factor (hSTAT3 or hPPARγ), Flag tagged human hormone receptor (ERα, VDR, THRβ or GR) or empty vector using lipofectamine 2000 (Invitrogen). Before harvest, cell were treated with leptin (at 200 ng/ml, 15 min, HARBOR-UCLA Research And Education Institute), or rosiglitazone (at 50 μM, ADIPOGEN), 17β-estradiol (at 0.2 μg/ml, Sigma, E2758), Vitamin D3 (Calcitriol at 0.2 μM, TOCRIS), dexamethasone (at 10 μM, Sigma, D4902) for 30 min. Cells were collected and lysed with cell lysis buffer: 50mM Tris, 50mM KCL, 10mM EDTA, 1% NP-40, supplied with protease inhibitor cocktail (Roche) and phosphatase inhibitor cocktail A (Santa Cruz). The lysates were incubated with proper amount of anti-phospho-STAT3 sepharose beads (Cellsignaling, #4074) or anti-Flag-beads (Sigma) for 4 h at 4^{o}C. After wash, beads were aliquoted equally and incubated with comparable amounts of SRC-1 protein (wt or mutants) overnight, and the interacting protein was detected by Western-Blot. SRC-1 WT or mutants were expressed in HEK293 cells and the amount of the SRC-1 expressed was determined by Western-Blot before the protein interaction assay. Comparable amounts of SRC-1 (wt or mutants) in the same volume of cell lysates (compensated with the cell lysates from the cells transfected with empty vector) were used for the in vitro protein interaction. Except for the THRβ IP were equal amounts of total protein from SRC-1 WT and mutant lysates (determined by bradford assay (Biorad)) were incubated with equal volumes of flag tagged

565 THRβ lysate overnight at 4°C with 1 μM T3 thyroid hormone. THRβ was then
566 immunoprecipitated using anti-Flag conjugated beads for 1h which were washed 6 times with
567 lysis buffer and eluted with LDS sample buffer before western blotting.
568
569 ***Luciferase transcription activation assays***
570 To measure STAT3 activity on the POMC promoter, HEK293, Neuro 2A (mouse neuroblastoma
571 cell line) and immortalized MEF cells (generated in J.X. lab) were cultured in Dulbecco's
572 modified Eagle's medium supplemented with 10% fetal bovine serum (Atlanta), 100 IU/ml
573 penicillin and 100 ng/ml streptomycin. Cells were seeded into a 24-well plate overnight and
574 then transfected with 600 ng of the Pomc-luciferase reporter plasmid[67] or 300 ng Socs3-
575 luciferase 6T1 reporter plasmid[12], combined with 100 ng of pRL-SV40 (Promega), 100 ng of
576 pCR3.1-SRC-1 and/or 10 ng pRc/CMV-STAT3C plasmids or the control empty plasmids,
577 according to the Lipofectamine LTX protocol (Invitrogen). Thirty hours post-transfection, the
578 cells were lysed and the luciferase activity was measured using the Dual-Luciferase® Reporter
579 Assay System (Promega) according to the manufacturer's instruction.
580
581 For leptin induced Pomc-luciferase reporter assay, a fragment of the human POMC promoter
582 (-949 to +416, relative to the transcription start site) was cloned into the pGL3 Luciferase
583 Reporter Vector by using the primer pairs: 5'- TGTTCTAGTTGGGGGAACAGC-3' and 5'-
584 GCGCCCTTACCTGTCTCGG-3'. Neuro 2A cells were cultured in 48-well plate for overnight and
585 then transfected with 0.1 μg human Pomc-luciferase reporter plasmid, 0.025 μg LepR and
586 0.05 μg hSRC-1 plasmid. Forty hours post-transfection, the cells were treated with 0.2 μg /ml
587 Leptin for 20 min and then kept cultured in fresh media for 6 h. To test the effect of dominant
588 negative STAT3 on leptin induced POMC-luciferase reporter activity, the above protocol was

589 modified by cotransfecting 10 ng of the dominant negative form of STAT3 (Y705F).

590

591 ***Human studies***

592 The Genetics of Obesity Study (GOOS) is a cohort of 7,000 individuals with severe early-onset
593 obesity; age of obesity onset is less than 10 years[68, 69]. Severe obesity is defined as a body
594 mass index (weight in kilograms divided by the square of the height in meters) standard
595 deviation score greater than 3 (standard deviation scores calculated according to the United
596 Kingdom reference population). All studies were conducted in accordance with ethical
597 regulations. The study protocol was reviewed and approved by the Cambridge Local Research
598 Ethics Committee and each subject (or their parent for those under 16 years) provided written
599 informed consent; minors provided oral consent.

600

601 Exome sequencing and targeted resequencing was performed in 2,548 European ancestry
602 individuals of the GOOS cohort (referred to as SCOOP) and in 1,117 ancestry-matched
603 controls16. Eleven rare variants (minor allele frequency<1%) in SRC-1 were identified in this
604 study16; another 8 variants were identified in an earlier data release. Fifteen of these rare
605 variants were identified in severely obese cases and 4 in the control dataset.

606

607 ***Quantification and statistical analysis***

608 The minimal sample size was pre-determined by the nature of experiments. The actual sample
609 size was indicated in each figure legend. The data are presented as mean ± SEM. Statistical
610 analyses were performed using GraphPad Prism to evaluate normal distribution and
611 variations within and among groups. Methods of statistical analyses were chosen based on

612 the design of each experiment and are indicated in figure legends. P<0.05 was considered to
613 be statistically significant.
614
615 **Data availability:** The source data underlying Figs 1-4 and Supplementary Figs 1-4 are
616 provided as Source Data files.

Reference

1. Dasgupta S, Lonard DM, O'Malley BW. Nuclear receptor coactivators: master regulators of human health and disease. *Annu Rev Med* **65**, 279-292 (2014).

2. York B, O'Malley BW. Steroid receptor coactivator (SRC) family: masters of systems biology. *The Journal of biological chemistry* **285**, 38743-38750 (2010).

3. Picard F*, et al.* SRC-1 and TIF2 control energy balance between white and brown adipose tissues. *Cell* **111**, 931-941 (2002).

4. Zhu L*, et al.* Steroid receptor coactivator-1 mediates estrogenic actions to prevent body weight gain in female mice. *Endocrinology* **154**, 150-158 (2013).

5. Hill JW, Elmquist JK, Elias CF. Hypothalamic pathways linking energy balance and reproduction. *Am J Physiol Endocrinol Metab* **294**, E827-832 (2008).

6. Morton GJ, Schwartz MW. Leptin and the central nervous system control of glucose metabolism. *Physiol Rev* **91**, 389-411 (2011).

7. Ahima RS*, et al.* Role of leptin in the neuroendocrine response to fasting. *Nature* **382**, 250-252 (1996).

8. Cowley MA*, et al.* Leptin activates anorexigenic POMC neurons through a neural network in the arcuate nucleus. *Nature* **411**, 480-484 (2001).

9. Xu AW, Ste-Marie L, Kaelin CB, Barsh GS. Inactivation of signal transducer and activator of transcription 3 in proopiomelanocortin (Pomc) neurons causes decreased pomc expression, mild obesity, and defects in compensatory refeeding. *Endocrinology* **148**, 72-80 (2007).

10. Bates SH*, et al.* STAT3 signalling is required for leptin regulation of energy balance but not reproduction. *Nature* **421**, 856-859 (2003).

11. Munzberg H, Huo L, Nillni EA, Hollenberg AN, Bjorbaek C. Role of signal transducer and activator of transcription 3 in regulation of hypothalamic proopiomelanocortin gene expression by leptin. *Endocrinology* **144**, 2121-2131 (2003).

12. Auernhammer CJ, Bousquet C, Melmed S. Autoregulation of pituitary corticotroph SOCS-3 expression: characterization of the murine SOCS-3 promoter. *Proc Natl Acad Sci U S A* **96**, 6964-6969 (1999).

13. Baskin DG, Breininger JF, Schwartz MW. SOCS-3 expression in leptin-sensitive neurons of the hypothalamus of fed and fasted rats. *Regul Pept* **92**, 9-15 (2000).

14. Giraud S, Bienvenu F, Avril S, Gascan H, Heery DM, Coqueret O. Functional interaction of STAT3 transcription factor with the coactivator NcoA/SRC1a. *The Journal of biological chemistry* **277**, 8004-8011 (2002).

15. Xu J, Qiu Y, DeMayo FJ, Tsai SY, Tsai MJ, O'Malley BW. Partial hormone resistance in mice with disruption of the steroid receptor coactivator-1 (SRC-1) gene. *Science* **279**, 1922-1925 (1998).

16. Padilla SL, Carmody JS, Zeltser LM. Pomc-expressing progenitors give rise to antagonistic neuronal populations in hypothalamic feeding circuits. *Nat Med* **16**, 403-405 (2010).

17. Berglund ED*, et al.* Serotonin 2C receptors in pro-opiomelanocortin neurons regulate energy and glucose homeostasis. *J Clin Invest* **123**, 5061-5070 (2013).

18. Myers MG, Jr., Leibel RL, Seeley RJ, Schwartz MW. Obesity and leptin resistance: distinguishing cause from effect. *Trends Endocrinol Metab* **21**, 643-651 (2010).

19. Caron A*, et al.* POMC neurons expressing leptin receptors coordinate metabolic responses to fasting via suppression of leptin levels. *eLife* **7**, (2018).

20. Xu J*, et al.* Genetic identification of leptin neural circuits in energy and glucose homeostases. *Nature* **556**, 505-509 (2018).

21. Beutler LR, Chen Y, Ahn JS, Lin YC, Essner RA, Knight ZA. Dynamics of Gut-Brain Communication Underlying Hunger. *Neuron* **96**, 461-475 e465 (2017).

22. Vong L, Ye C, Yang Z, Choi B, Chua S, Jr., Lowell BB. Leptin action on GABAergic neurons prevents obesity and reduces inhibitory tone to POMC neurons. *Neuron* **71**, 142-154 (2011).

23. Pinto S*, et al.* Rapid rewiring of arcuate nucleus feeding circuits by leptin. *Science* **304**, 110-115 (2004).

24. Hendricks AE*, et al.* Rare Variant Analysis of Human and Rodent Obesity Genes in Individuals with Severe Childhood Obesity. *Scientific reports* **7**, 4394 (2017).

25. Caron A*, et al.* POMC neurons expressing leptin receptors coordinate metabolic responses to fasting via suppression of leptin levels. *Elife* **7**, (2018).

26. van de Wall E*, et al.* Collective and individual functions of leptin receptor modulated neurons controlling metabolism and ingestion. *Endocrinology* **149**, 1773-1785 (2008).

27. Balthasar N*, et al.* Leptin receptor signaling in POMC neurons is required for normal body weight homeostasis. *Neuron* **42**, 983-991 (2004).

28. Yaswen L, Diehl N, Brennan MB, Hochgeschwender U. Obesity in the mouse model of pro-opiomelanocortin deficiency responds to peripheral melanocortin. *Nature medicine* **5**, 1066-1070 (1999).

29. Huszar D*, et al.* Targeted disruption of the melanocortin-4 receptor results in obesity in mice. *Cell* **88**, 131-141 (1997).

30. Hartmaier RJ, *et al.* A SNP in steroid receptor coactivator-1 disrupts a GSK3beta phosphorylation site and is associated with altered tamoxifen response in bone. *Mol Endocrinol* **26**, 220-227 (2012).

31. Leshan RL, Greenwald-Yarnell M, Patterson CM, Gonzalez IE, Myers MG, Jr. Leptin action through hypothalamic nitric oxide synthase-1-expressing neurons controls energy balance. *Nat Med* **18**, 820-823 (2012).

32. Morton GJ, Gelling RW, Niswender KD, Morrison CD, Rhodes CJ, Schwartz MW. Leptin regulates insulin sensitivity via phosphatidylinositol-3-OH kinase signaling in mediobasal hypothalamic neurons. *Cell Metab* **2**, 411-420 (2005).

33. Blouet C, Ono H, Schwartz GJ. Mediobasal hypothalamic p70 S6 kinase 1 modulates the control of energy homeostasis. *Cell Metab* **8**, 459-467 (2008).

34. Minokoshi Y, *et al.* AMP-kinase regulates food intake by responding to hormonal and nutrient signals in the hypothalamus. *Nature* **428**, 569-574 (2004).

35. Dagon Y, Hur E, Zheng B, Wellenstein K, Cantley LC, Kahn BB. p70S6 kinase phosphorylates AMPK on serine 491 to mediate leptin's effect on food intake. *Cell Metab* **16**, 104-112 (2012).

36. Spencer TE, *et al.* Steroid receptor coactivator-1 is a histone acetyltransferase. *Nature* **389**, 194-198 (1997).

37. Zhang X, Zhang G, Zhang H, Karin M, Bai H, Cai D. Hypothalamic IKKbeta/NF-kappaB and ER stress link overnutrition to energy imbalance and obesity. *Cell* **135**, 61-73 (2008).

38. Ozcan L, *et al.* Endoplasmic reticulum stress plays a central role in development of leptin resistance. *Cell Metab* **9**, 35-51 (2009).

39. Kaneko K, *et al.* Neuronal Rap1 Regulates Energy Balance, Glucose Homeostasis, and Leptin Actions. *Cell Rep* **16**, 3003-3015 (2016).

40. Schneeberger M, *et al.* Mitofusin 2 in POMC neurons connects ER stress with leptin resistance and energy imbalance. *Cell* **155**, 172-187 (2013).

41. Diano S, *et al.* Peroxisome proliferation-associated control of reactive oxygen species sets melanocortin tone and feeding in diet-induced obesity. *Nat Med* **17**, 1121-1127 (2011).

42. Thaler JP, *et al.* Obesity is associated with hypothalamic injury in rodents and humans. *J Clin Invest* **122**, 153-162 (2012).

43. Chen Y, *et al.* Enhancement of hypothalamic STAT3 acetylation by nuclear receptor Nur77 dictates leptin sensitivity. *Diabetes* **64**, 2069-2081 (2015).

44. Xu Y, O'Malley BW, Elmquist JK. Brain nuclear receptors and body weight regulation. *J Clin Invest* **127**, 1172-1180 (2017).

45. Plum L, *et al.* The obesity susceptibility gene Cpe links FoxO1 signaling in hypothalamic pro-opiomelanocortin neurons with regulation of food intake. *Nat Med* **15**, 1195-1201 (2009).

46. Kitamura T, *et al.* Forkhead protein FoxO1 mediates Agrp-dependent effects of leptin on food intake. *Nat Med* **12**, 534-540 (2006).

47. Kim MS, *et al.* Role of hypothalamic Foxo1 in the regulation of food intake and energy homeostasis. *Nat Neurosci* **9**, 901-906 (2006).

48. Ren H, *et al.* FoxO1 Target Gpr17 Activates AgRP Neurons to Regulate Food Intake. *Cell* **149**, 1314-1326 (2012).

49. Xu Y, *et al.* Distinct hypothalamic neurons mediate estrogenic effects on energy homeostasis and reproduction. *Cell Metab* **14**, 453-465 (2011).

50. Musatov S, *et al.* Silencing of estrogen receptor alpha in the ventromedial nucleus of hypothalamus leads to metabolic syndrome. *Proc Natl Acad Sci U S A* **104**, 2501-2506 (2007).

51. Lu M, *et al.* Brain PPAR-gamma promotes obesity and is required for the insulin-sensitizing effect of thiazolidinediones. *Nat Med* **17**, 618-622 (2011).

52. Ryan KK, Li B, Grayson BE, Matter EK, Woods SC, Seeley RJ. A role for central nervous system PPAR-gamma in the regulation of energy balance. *Nat Med* **17**, 623-626 (2011).

53. Lopez M, *et al.* Hypothalamic AMPK and fatty acid metabolism mediate thyroid regulation of energy balance. *Nat Med* **16**, 1001-1008 (2010).

54. Lonard DM, O'Malley BW. Molecular Pathways: Targeting Steroid Receptor Coactivators in Cancer. *Clin Cancer Res* **22**, 5403-5407 (2016).

55. Wang L, *et al.* Characterization of a Steroid Receptor Coactivator Small Molecule Stimulator that Overstimulates Cancer Cells and Leads to Cell Stress and Death. *Cancer Cell* **28**, 240-252 (2015).

56. Shang Y, Brown M. Molecular determinants for the tissue specificity of SERMs. *Science* **295**, 2465-2468 (2002).

57. Farooqi IS, *et al.* Effects of recombinant leptin therapy in a child with congenital leptin deficiency. *N Engl J Med* **341**, 879-884 (1999).

58. Oral EA, *et al.* Leptin-replacement therapy for lipodystrophy. *N Engl J Med* **346**, 570-578 (2002).

59. Flier JS, Maratos-Flier E. Leptin's Physiologic Role: Does the Emperor of Energy Balance Have No Clothes? *Cell Metab* **26**, 24-26 (2017).

60. Konner AC, Bruning JC. Selective insulin and leptin resistance in metabolic disorders. *Cell Metab* **16**, 144-152 (2012).

61. Friedman J. The long road to leptin. *J Clin Invest* **126**, 4727-4734 (2016).

62. Li Z, Kelly L, Heiman M, Greengard P, Friedman JM. Hypothalamic Amylin Acts in Concert with Leptin to Regulate Food Intake. *Cell Metab* **22**, 1059-1067 (2015).

63. Roth JD*, et al.* Leptin responsiveness restored by amylin agonism in diet-induced obesity: evidence from nonclinical and clinical studies. *Proc Natl Acad Sci U S A* **105**, 7257-7262 (2008).

64. Yamada T*, et al.* SRC-1 is necessary for skeletal responses to sex hormones in both males and females. *Journal of bone and mineral research : the official journal of the American Society for Bone and Mineral Research* **19**, 1452-1461 (2004).

65. Bassett AR, Tibbit C, Ponting CP, Liu JL. Highly efficient targeted mutagenesis of Drosophila with the CRISPR/Cas9 system. *Cell Rep* **4**, 220-228 (2013).

66. Winnay JN, Xu J, O'Malley BW, Hammer GD. Steroid receptor coactivator-1-deficient mice exhibit altered hypothalamic-pituitary-adrenal axis function. *Endocrinology* **147**, 1322-1332 (2006).

67. Zhang H, Zhang G, Gonzalez FJ, Park SM, Cai D. Hypoxia-inducible factor directs POMC gene to mediate hypothalamic glucose sensing and energy balance regulation. *PLoS Biol* **9**, e1001112 (2011).

68. Farooqi IS, Keogh JM, Yeo GS, Lank EJ, Cheetham T, O'Rahilly S. Clinical spectrum of obesity and mutations in the melanocortin 4 receptor gene. *N Engl J Med* **348**, 1085-1095 (2003).

69. Wheeler E*, et al.* Genome-wide SNP and CNV analysis identifies common and low-frequency variants associated with severe early-onset obesity. *Nat Genet* **45**, 513-517 (2013).

852 **Author contributions:** YY, AAvdK, YX and ISF conceived and designed the studies; YX and ISF
853 supervised the project; YY and LZ performed and CW, PX, KS, AHJ, XY, LL, JX contributed to
854 the experiments involving animals; YH performed electrophysiological studies; QT and BO'M
855 participated in the design of the animal studies. AAvdK, TC, JMK, EH contributed to the human
856 studies and with SOR and ISF to the recruitment of the GOOS cohort; TC, LKJS and MCB
857 performed the molecular studies of human mutations; AEH, EGB, VM, KLL, IB and ISF
858 contributed to the human genetic studies as part of work supported by the UK10K
859 consortium.

860

861 **Acknowledgements:** Studies in cells and animals were supported by grants from the NIH
862 (R01DK093587, R01DK101379 and R01DK117281 to YX; R01DK114279 to QT, R01CA112403
863 and R01CA193455 to JX; R01HD07857, R01HD008818 and P01DK059820 to BWO;
864 P0101DK113954 to YX, JX and BWO), USDA/CRIS (6250-51000-059-04S to YX), American Heart
865 Association (to QT and YX), Chinese National Natural Science Foundation (NSFC 81873558 to
866 LZ). This work was partially supported by the Cancer Prevention and Research Institute of
867 Texas (RP170005) and the NCI Cancer Center Support Grant (P30CA125123). Measurements
868 of body composition, food intake and energy expenditure in mice were performed in the
869 Mouse Metabolic Research Unit (MMRU) at the USDA/ARS Children's Nutrition Research
870 Center, Baylor College of Medicine, which is supported by funds from the USDA ARS
871 (www.bcm.edu/cnrc/mmru). The *Pomc-CreER* mouse line was provided by Dr. Joel Elmquist
872 (University of Texas Southwestern Medical Center); the *SRC-1*$^{lox/lox}$ mouse line was provided
873 by Dr. Pierre Chambon (IGBMC/GIE-CERBM). The authors thank BCM Mouse Embryonic Stem
874 Cell Core and Genetically Engineered Mouse Core for their assistance in generating the SRC-

1^{L1376P} knock-in mouse. The authors acknowledge the expert assistance of Mr. Firoz Vohra and the MMRU Core Director, Dr. Marta Fiorotto. Studies in humans were supported by the Wellcome Trust (AAvdK, TMC, IB, ISF) (098497/Z/12/Z; WT098051; 203513/Z/16/Z), NIHR Cambridge Biomedical Research Centre (ISF, IB, SOR), Bernard Wolfe Health Neuroscience Endowment (ISF). TMC was supported by a Philip Greenwood Clinical Research Fellowship and a Wellcome Trust Research Training Fellowship. We are indebted to the participants and their families for their participation and to the Physicians involved in the Genetics of Obesity Study (GOOS) (www.goos.org.uk); whole-exome sequencing was performed as part of the UK10K consortium (a full list of investigators who contributed to the generation of the data is available from www.UK10K.org.uk)."

Authors have no conflict of interest to disclose.

887 **Figure Legends**

888 **Figure 1. SRC-1 potentiates STAT3-induced Pomc expression.**

889 Numbers of mice/repeats in each group are indicated; data are presented as mean ± SEM and
890 compared using T-tests or two-way ANOVA followed by post hoc Sidak tests (#). (a) Pomc and
891 Socs3 mRNA levels in hypothalami from 16-week old *SRC-1-KO* and WT control littermates
892 (n=7/8); *** P<0.001. (b) ChIP assays detecting pSTAT3 binding on *Pomc* promoters in
893 hypothalami from male *SRC-1-KO* and control littermates 30 min after leptin injections (5
894 mg/kg, i.p.): site 1, -998 to -989; site 2, -361 to -353; site 3, -76 to -68 upstream of *Pomc*
895 (n=3/4); * P<0.05. (c-d) Effects of overexpressed constitutively active STAT3 and SRC-1 on
896 Pomc- (c) or Socs3-luciferase activity (d) in Neuro2A cells (n=5-9 independent experiments).
897 *** P<0.001 vs. empty vectors; ### P<0.001 vs. STAT3 alone (#). (e) Change (Δ) in body weight
898 after male control and pomcSRC-1-KO mice were switched onto a HFD at day 97 (n=6/9); *
899 P<0.05 and ** P<0.01 (#). (f) Fat mass and lean mass measured 28 days after HFD feeding
900 (n=6/9); * P<0.05. (g) Energy intake measured by CLAMS chambers in 12-week old male mice
901 matched for body weight, lean mass and fat mass. Mice were subjected to a 2-day-chow-2-
902 day-HFD protocol, and chow was replaced by HFD before the onset of dark cycle on day 3.
903 Energy intake was averaged for 2-day chow feeding period and for 2-day HFD feeding period
904 (n=7/8); * P<0.05. (h) Cumulative HFD intake measured in 12-week old male mice singly
905 housed in home cages (n=10/14); * P<0.05 (#). (i) Change in body weight after control and
906 MpomcSRC-1-KO mice were switched on a HFD at the age of day 84 (n=8); * P<0.05 (#). (j) Fat
907 mass and lean mass measured 30 days after HFD feeding (n=8); *P<0.05. (k) Cumulative HFD
908 intake measured in 12-week old male mice (n=6/7); * P<0.05 (#). **Source data are provided**
909 **as Source Data Fig 1.xlsx.**

Figure 2. SRC-1 mediates leptin signaling

Numbers of mice/experiments/neurons are indicated; data are presented as mean ± SEM and compared using T-tests or one- or two-way ANOVA followed by post hoc Sidak tests (#). (a) Serum leptin levels 42 days after HFD feeding (n=5/8); * P<0.05. (b) Time course of hypothalamic SRC-1-pSTAT3 interaction in C57Bl6 wild type mice that received i.p. injections of leptin (5 mg/kg). (c) Quantification of the hypothalamic SRC-1-pSTAT3 interaction. * P<0.05 (#). (d) Two-hour fasted mice (12 weeks of age) received i.p. injections of saline or leptin (5 mg/kg) 15 min prior to refeeding and food intake was record for 1 hour afterwards (n=7/9); ** P<0.01 (#). (e) Representative pSTAT3 immunohistochemical staining in the ARH and VMH of control and pomcSRC-1-KO mice receiving a single bolus i.p. injection of leptin (0.5 mg/kg, 90 min). Scale bar = 50 µm. 3V, the 3rd ventricle; ARH, arcuate nucleus; VMH, ventromedial hypothalamic nucleus. (f) Quantification of pSTAT3 (+) neurons in the ARH (n=5); *** P<0.001. (g) Representative traces of leptin-induced depolarization, in the presence of TTX, CNQX, DAP-5 and bicuculline, in mature Pomc neurons from control mice vs. from MpomcSRC-1-KO mice after one-week HFD feeding. (h) Responsive ratio (depolarization is defined as >2 mV elevations in resting membrane potential) (n=39/43); P=0.002 in $\chi 2$ tests. (i) Quantification of leptin-induced depolarization in two groups (n=39/43); ** P<0.01. (j) Representative traces of action potentials in untreated mature Pomc neurons from control mice vs. from MpomcSRC-1-KO mice. (k-l) Quantification of firing frequency (k) and resting membrane potential (l) in two groups (n=29-36); * P<0.05. (m) Representative traces of mIPSC in untreated mature Pomc neurons from control mice vs. from MpomcSRC-1-KO mice. (n-o) Quantification of amplitude (n) and frequency (o) of mIPSC in two groups (n=13/14); ***

P<0.001. **Source data are provided as Source Data Fig 2.xlsx, Source Data Fig 2e Control.tif and Source Data Fig 2e pomcSRC-1-KO.tif.**

Figure 3. Missense variants in SRC-1 disrupt leptin signalling

Numbers of experiments are indicated; data are presented as mean ± SEM and compared using one-way ANOVA followed by post hoc Sidak tests unless mentioned otherwise. (a) Rare variants identified in individuals with severe early onset obesity (above) and in controls (below). (b-c) HEK293 cells were co-transfected with leptin receptor vector and human STAT3 vector. Cells were treated with leptin (200 ng/ml, 15 min) to induce phosphorylation of STAT3. pSTAT3 was pulled down using anti-pSTAT3 sepharose beads; beads were then aliquoted equally and incubated with the same amount of the long isoform of human SRC-1-HA (WT/mutant) and interactions between the pSTAT3 and SRC-1 were determined by CoIP experiments using anti-pSTAT3 and anti-HA antibodies. (b) Representative blots showing interactions between pSTAT3 and SRC-1 (WT/mutant), and inputs of pSTAT3 and SRC-1-HA. (c) Quantification for WT and SRC-1 mutants. Comparative folds were calculated as the ratios of HA blots and HA inputs (n=3-5); * P<0.05. (d-e) SRC-1 mutants inhibit interaction between STAT3 and WT SRC-1. HEK293 cells were co-transfected with leptin receptor vector, STAT3 vector, and mutant SRC-1 vector (or empty vector). Cells were treated with leptin (200 ng/ml, 15 min) to induce phosphorylation of STAT3 and interactions between pSTAT3 and total SRC-1 were determined by CoIP experiments using anti-pSTAT3 and anti-SRC-1 antibodies. (d) Representative blots showing interactions between pSTAT3 and SRC-1 variants found in obese cases and inputs of pSTAT3. (e) Quantification. Comparative folds were calculated as the ratios of SRC-1-pSTAT3 interaction blots and pSTAT3 inputs (n=4-12); * P<0.05. (f) SRC-1

variants impair POMC expression. Neuro2A cells were co-transfected with leptin receptor vector, SRC-1 (WT or mutant) and a POMC luciferase expression reporter construct. Cells were stimulated with 200ng/ml leptin for 15 minutes and then incubated for 6 hours, following which luminescence was measured. Results were normalized to empty vector-induced expression (n=3-16); * P<0.05. **Source data are provided as Source Data Fig 3.xlsx.**

Figure 4. *SRC-1*$^{L1376P/+}$ mice are obese.

Numbers of mice in each group are indicated; data are presented as mean ± SEM and compared using T-tests or two-way ANOVA followed by post hoc Sidak tests (#). (a) The PCR products (121 bp) around the L1376 were amplified from genomic DNA extracts of a WT and two *SRC-1*$^{L1376P/+}$ mutant mice and incubated with or without Sau3AI. Control reaction (WT) resulted in a single large fragment (121 bp) and DNAs from the two *SRC-1*$^{L1376P/+}$ mutant mice were cut into two fragments (70 and 51 bp) as expected. (b) Change in body weight after male control and SRC-1$^{L1376P/+}$ mice were fed on a HFD (n=5/6); * P<0.05 (#). (c) Fat mass and lean mass measured 7 weeks after HFD feeding (n=5/6); *** P<0.001. (d) Cumulative HFD intake measured (n=5/6); * P<0.05 or ** P<0.01 (#). (e) Pomc mRNA levels in hypothalami from 20-week old HFD-fed male control and SRC-1$^{L1376P/+}$ mice (n=12/16); * P<0.05. (f) Representative traces of leptin-induced depolarization, in the presence of TTX, CNQX, DAP-5 and bicuculline, in Pomc neurons from control mice vs. from *SRC-1*$^{L1376P/+}$ mice after one-week HFD feeding. (g) Responsive ratio (depolarization is defined as >2 mV elevations in resting membrane potential) (n=19); P=0.022 in $\chi 2$ tests. (h) Quantification of leptin-induced depolarization in two groups (n=19); *** P<0.001. (i) Representative traces of action potentials in untreated Pomc neurons from control mice vs. from *SRC-1*$^{L1376P/+}$ mice. (j-k) Quantification of firing frequency (j) and resting membrane potential (k) in two groups (n=22-28); *** P<0.001. (l)

Representative traces of mIPSC in untreated Pomc neurons from control mice vs. from *SRC-1*$^{L1376P/+}$ mice. (m-n) Quantification of amplitude (m) and frequency (n) of mIPSC in two groups (n=10/12); *** P<0.001. **Source data are provided as Source Data Fig 4.xlsx.**

Figure 1

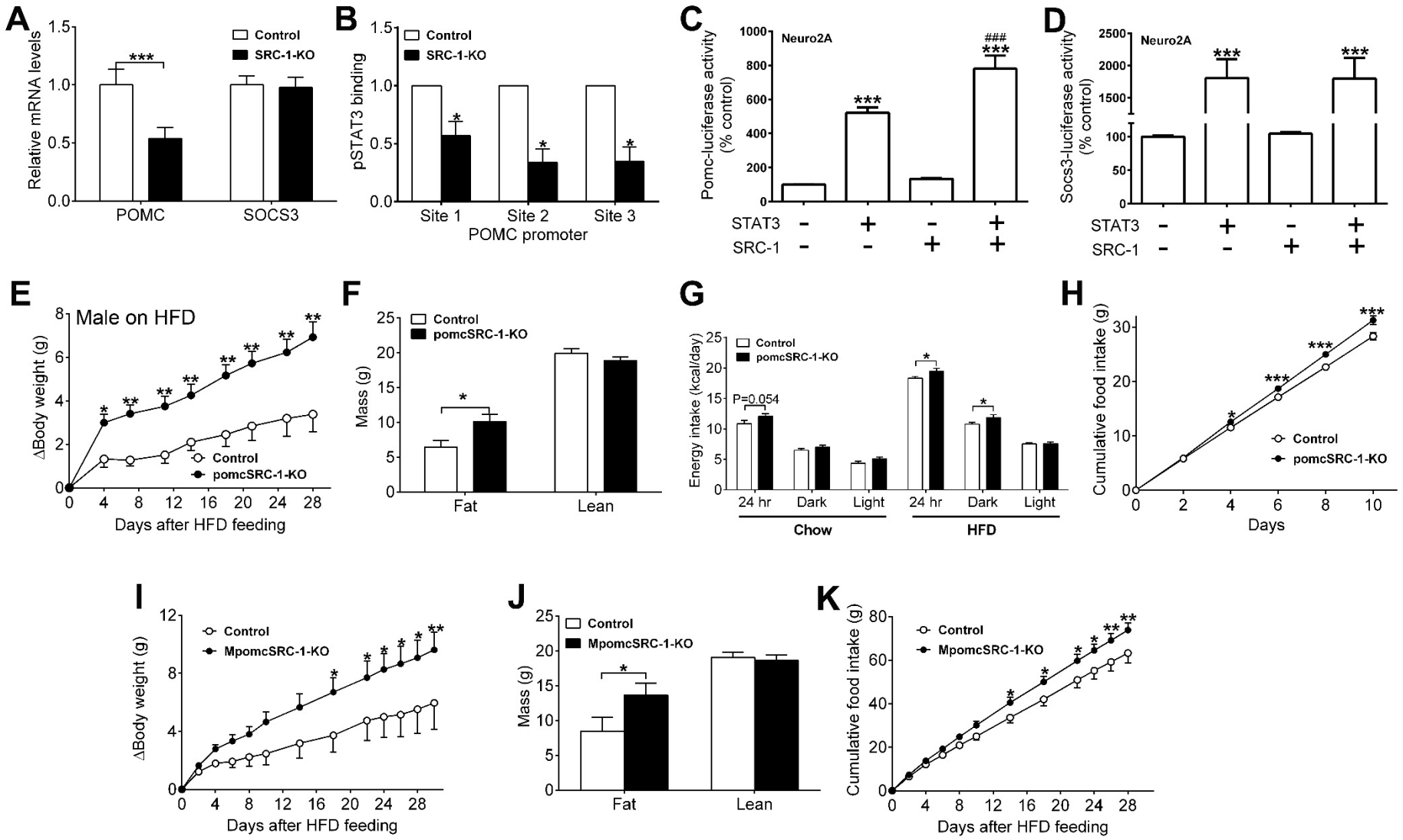
A
Relative mRNA levels
Control
SRC-1-KO
POMC
SOCS3
B
pSTAT3 binding
Site 1
Site 2
Site 3
POMC promoter
C
Neuro2A
Pomc-luciferase activity (% control)
STAT3
SRC-1
D
Neuro2A
Socs3-luciferase activity (% control)
STAT3
SRC-1
E
Male on HFD
ΔBody weight (g)
Days after HFD feeding
pomcSRC-1-KO
F
Mass (g)
Fat
Lean
G
Energy intake (kcal/day)
P=0.054
24 hr
Dark
Light
Chow
HFD
H
Cumulative food intake (g)
Days
I
ΔBody weight (g)
MpomcSRC-1-KO
Days after HFD feeding
J
Mass (g)
K
Cumulative food intake (g)
Days after HFD feeding

Figure 2

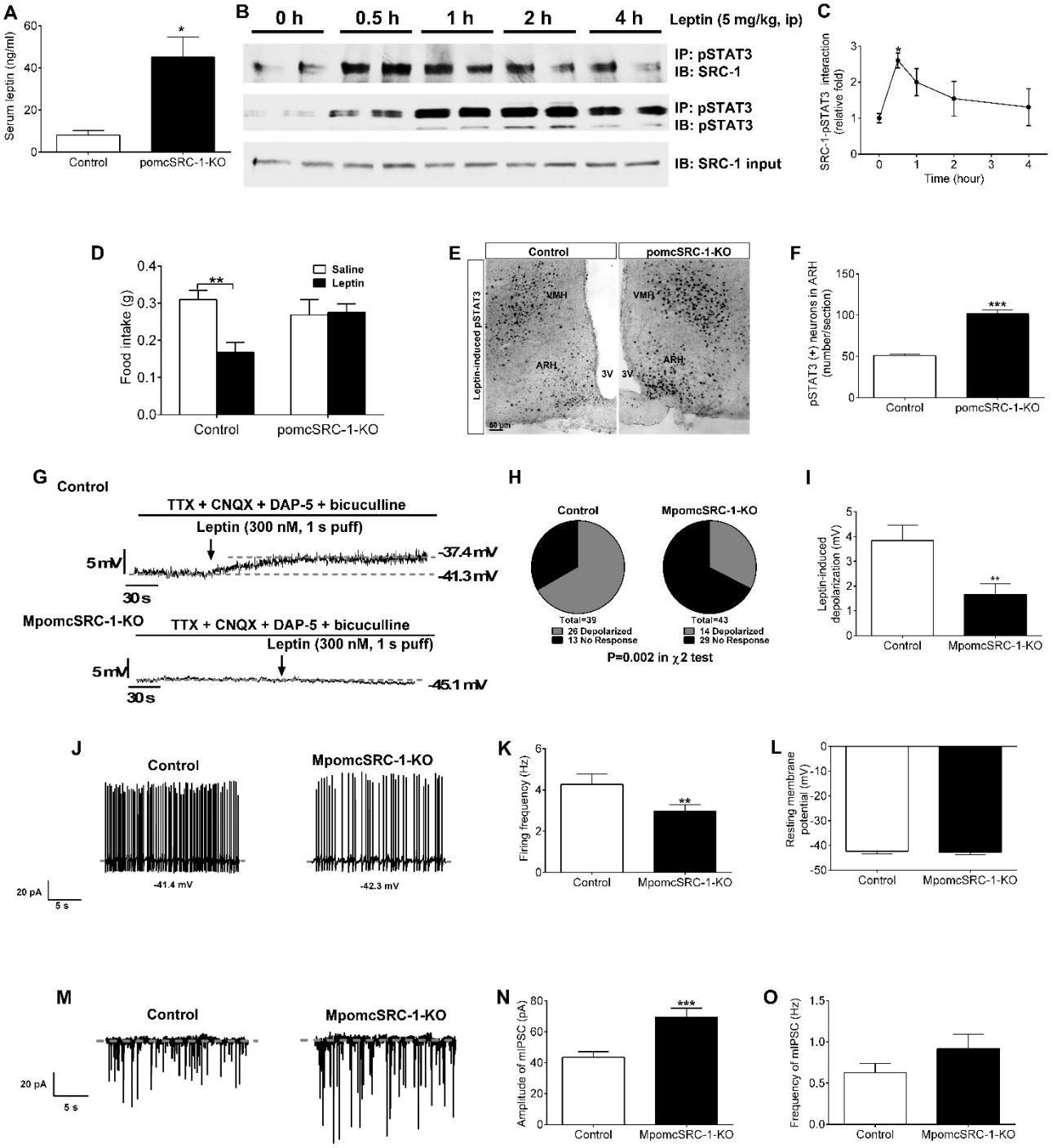
A
Serum leptin (ng/ml)
Control
pomcSRC-1-KO
B
0 h
0.5 h
1 h
2 h
4 h
Leptin (5 mg/kg, ip)
IP: pSTAT3
IB: SRC-1
IP: pSTAT3
IB: pSTAT3
IB: SRC-1 input
C
SRC-1-pSTAT3 interaction (relative fold)
Time (hour)
D
Food intake (g)
Saline
Leptin
Control
pomcSRC-1-KO
E
Control
pomcSRC-1-KO
Leptin-induced pSTAT3
VMH
ARH
3V
50 μm
F
pSTAT3 (+) neurons in ARH (number/section)
Control
pomcSRC-1-KO
G
Control
TTX + CNQX + DAP-5 + bicuculline
Leptin (300 nM, 1 s puff)
5 mV
30 s
-37.4 mV
-41.3 mV
MpomcSRC-1-KO
TTX + CNQX + DAP-5 + bicuculline
Leptin (300 nM, 1 s puff)
5 mV
30 s
-45.1 mV
H
Control
MpomcSRC-1-KO
Total=39
26 Depolarized
13 No Response
Total=43
14 Depolarized
29 No Response
P=0.002 in χ2 test
I
Leptin-induced depolarization (mV)
Control
MpomcSRC-1-KO
J
Control
MpomcSRC-1-KO
-41.4 mV
-42.3 mV
20 pA
5 s
K
Firing frequency (Hz)
Control
MpomcSRC-1-KO
L
Resting membrane potential (mV)
Control
MpomcSRC-1-KO
M
Control
MpomcSRC-1-KO
20 pA
5 s
N
Amplitude of mIPSC (pA)
Control
MpomcSRC-1-KO
O
Frequency of mIPSC (Hz)
Control
MpomcSRC-1-KO

Figure 3

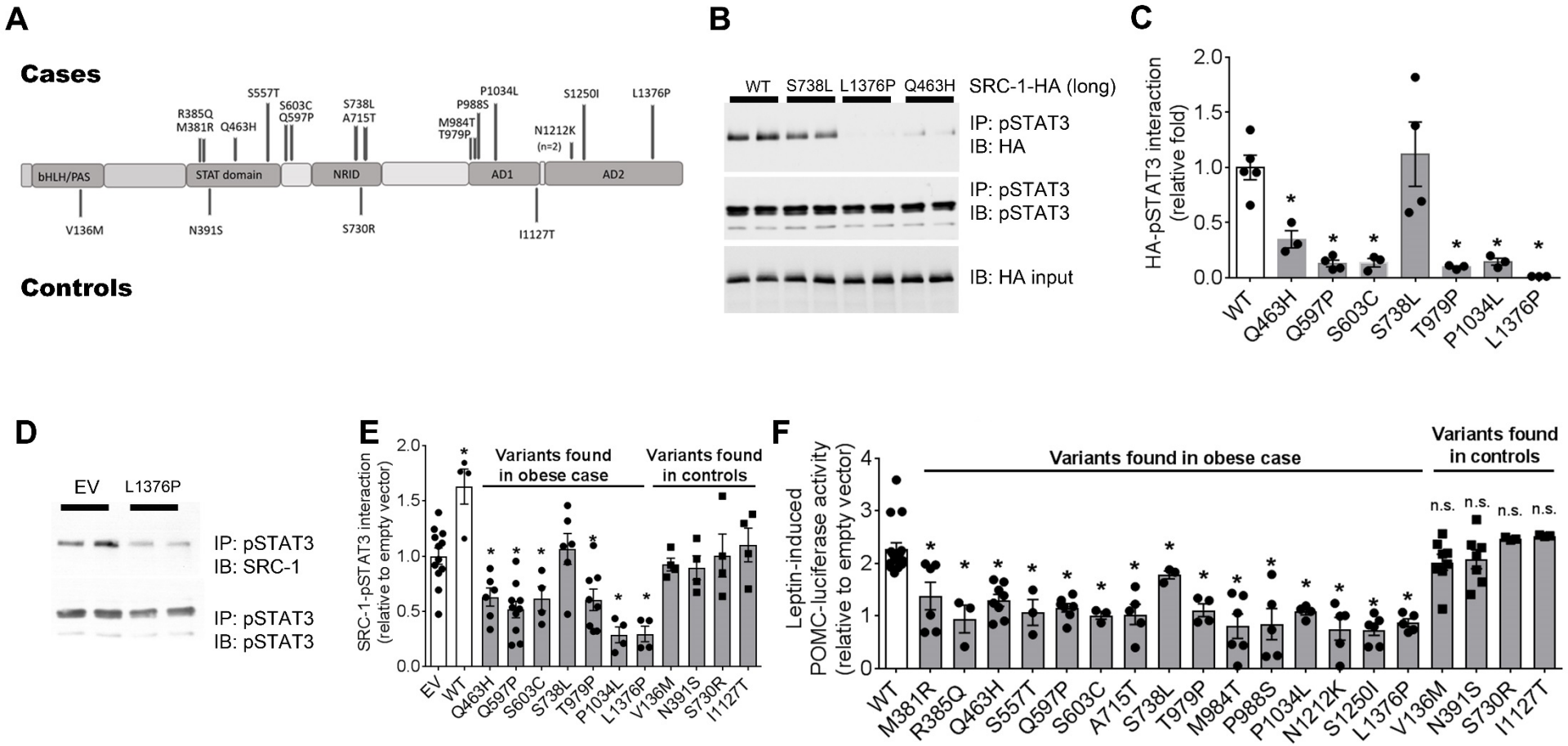
A
Cases
R385Q
M381R
Q463H
S557T
S603C
Q597P
S738L
A715T
M984T
T979P
P988S
P1034L
N1212K
(n=2)
S1250I
L1376P
bHLH/PAS
STAT domain
NRID
AD1
AD2
V136M
N391S
S730R
I1127T
Controls
B
WT
S738L
L1376P
Q463H
SRC-1-HA (long)
IP: pSTAT3
IB: HA
IP: pSTAT3
IB: pSTAT3
IB: HA input
C
HA-pSTAT3 interaction
(relative fold)
2.0
1.5
1.0
0.5
0.0
WT
Q463H
Q597P
S603C
S738L
T979P
P1034L
L1376P
D
EV
L1376P
IP: pSTAT3
IB: SRC-1
IP: pSTAT3
IB: pSTAT3
E
SRC-1-pSTAT3 interaction
(relative to empty vector)
2.0
1.5
1.0
0.5
0.0
Variants found
in obese case
Variants found
in controls
EV
WT
Q463H
Q597P
S603C
S738L
T979P
P1034L
L1376P
V136M
N391S
S730R
I1127T
F
Leptin-induced
POMC-luciferase activity
(relative to empty vector)
4
3
2
1
0
Variants found in obese case
Variants found
in controls
n.s.
n.s.
n.s.
n.s.
WT
M381R
R385Q
Q463H
S557T
Q597P
S603C
A715T
S738L
T979P
M984T
P988S
P1034L
N1212K
S1250I
L1376P
V136M
N391S
S730R
I1127T

Figure 4

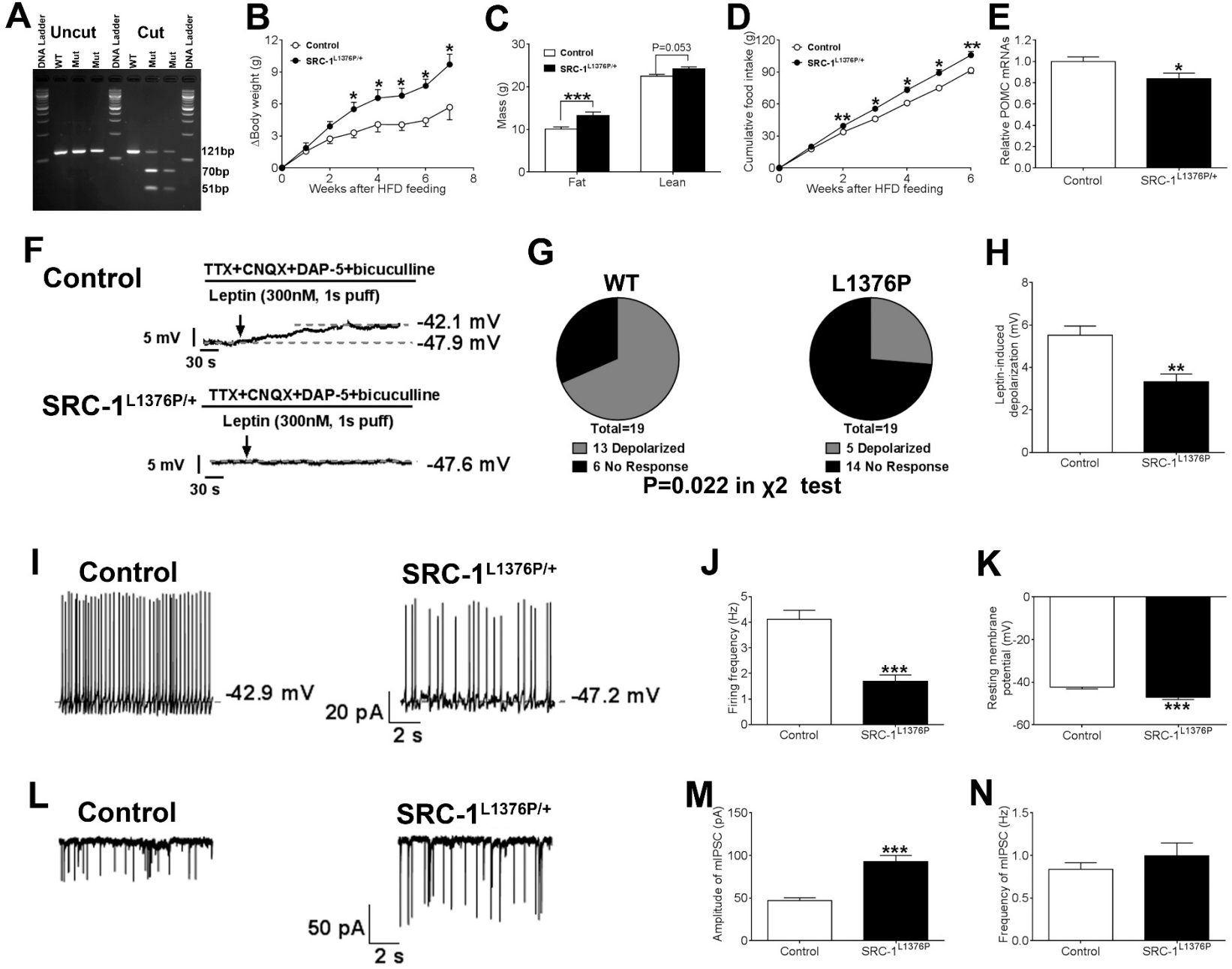
A
Uncut
Cut
DNA Ladder
WT
Mut
Mut
Mut
DNA Ladder
WT
Mut
Mut
DNA Ladder
121bp
70bp
51bp
B
Control
SRC-1L1376P/+
ΔBody weight (g)
Weeks after HFD feeding
C
Control
SRC-1L1376P/+
P=0.053
Mass (g)
***
Fat
Lean
D
Control
SRC-1L1376P/+
Cumulative food intake (g)
Weeks after HFD feeding
E
Relative POMC mRNAs
Control
SRC-1L1376P/+
F
Control
TTX+CNQX+DAP-5+bicuculline
Leptin (300nM, 1s puff)
5 mV
30 s
-42.1 mV
-47.9 mV
SRC-1L1376P/+
TTX+CNQX+DAP-5+bicuculline
Leptin (300nM, 1s puff)
5 mV
30 s
-47.6 mV
G
WT
L1376P
Total=19
13 Depolarized
6 No Response
Total=19
5 Depolarized
14 No Response
P=0.022 in χ2 test
H
Leptin-induced depolarization (mV)
Control
SRC-1L1376P
I
Control
SRC-1L1376P/+
-42.9 mV
-47.2 mV
20 pA
2 s
J
Firing frequency (Hz)
Control
SRC-1L1376P
K
Resting membrane potential (mV)
Control
SRC-1L1376P
L
Control
SRC-1L1376P/+
50 pA
2 s
M
Amplitude of mIPSC (pA)
Control
SRC-1L1376P
N
Frequency of mIPSC (Hz)
Control
SRC-1L1376P

Figure S1

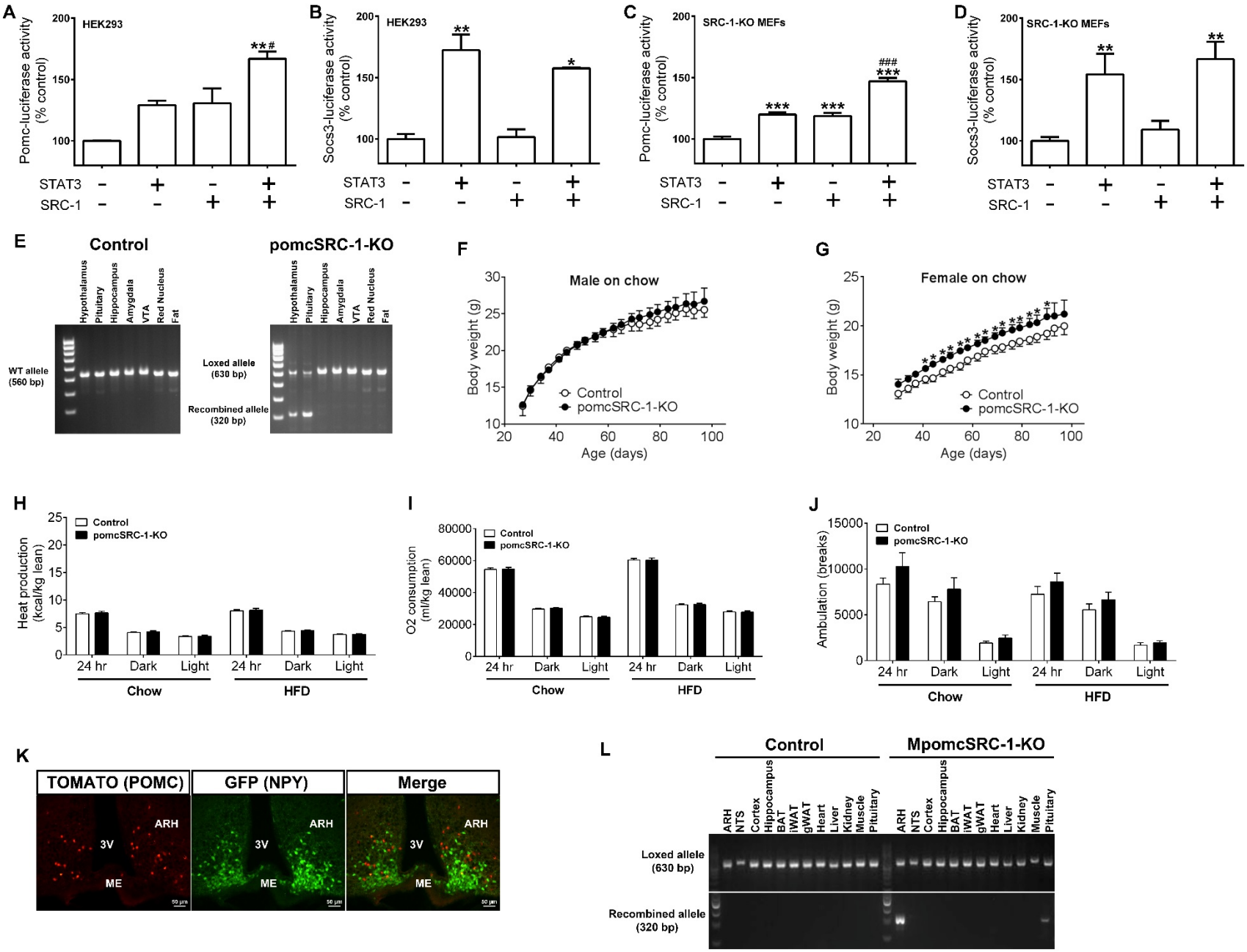
A
HEK293
Pomc-luciferase activity (% control)
STAT3
SRC-1
B
HEK293
Socs3-luciferase activity (% control)
C
SRC-1-KO MEFs
Pomc-luciferase activity (% control)
D
SRC-1-KO MEFs
Socs3-luciferase activity (% control)
E
Control
pomcSRC-1-KO
Hypothalamus
Pituitary
Hippocampus
Amygdala
VTA
Red Nucleus
Fat
WT allele (560 bp)
Loxed allele (630 bp)
Recombined allele (320 bp)
F
Male on chow
Body weight (g)
Age (days)
Control
pomcSRC-1-KO
G
Female on chow
H
Heat production (kcal/kg lean)
24 hr
Dark
Light
Chow
HFD
I
O2 consumption (ml/kg lean)
J
Ambulation (breaks)
K
TOMATO (POMC)
GFP (NPY)
Merge
ARH
3V
ME
L
Control
MpomcSRC-1-KO
ARH
NTS
Cortex
Hippocampus
BAT
iWAT
gWAT
Heart
Liver
Kidney
Muscle
Pituitary
Loxed allele (630 bp)
Recombined allele (320 bp)

Figure S2

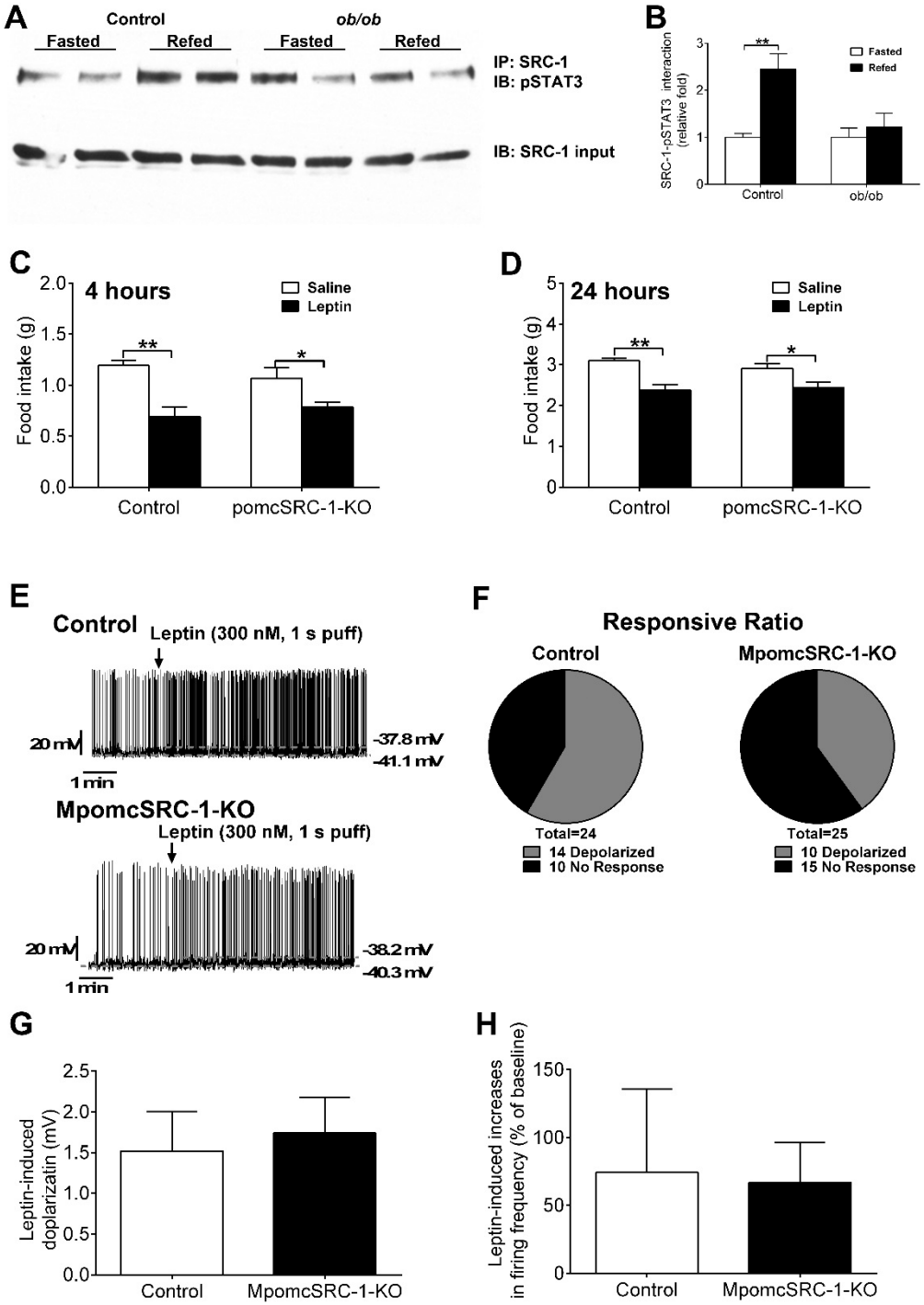
A
Control
ob/ob
Fasted
Refed
Fasted
Refed
IP: SRC-1
IB: pSTAT3
IB: SRC-1 input
B
SRC-1-pSTAT3 interaction (relative fold)
Fasted
Refed
Control
ob/ob
C
4 hours
Saline
Leptin
Food intake (g)
Control
pomcSRC-1-KO
D
24 hours
Saline
Leptin
Food intake (g)
Control
pomcSRC-1-KO
E
Control
Leptin (300 nM, 1 s puff)
20 mV
1 min
-37.8 mV
-41.1 mV
MpomcSRC-1-KO
Leptin (300 nM, 1 s puff)
20 mV
1 min
-38.2 mV
-40.3 mV
F
Responsive Ratio
Control
MpomcSRC-1-KO
Total=24
14 Depolarized
10 No Response
Total=25
10 Depolarized
15 No Response
G
Leptin-induced doplarizatin (mV)
Control
MpomcSRC-1-KO
H
Leptin-induced increases in firing frequency (% of baseline)
Control
MpomcSRC-1-KO

Figure S3

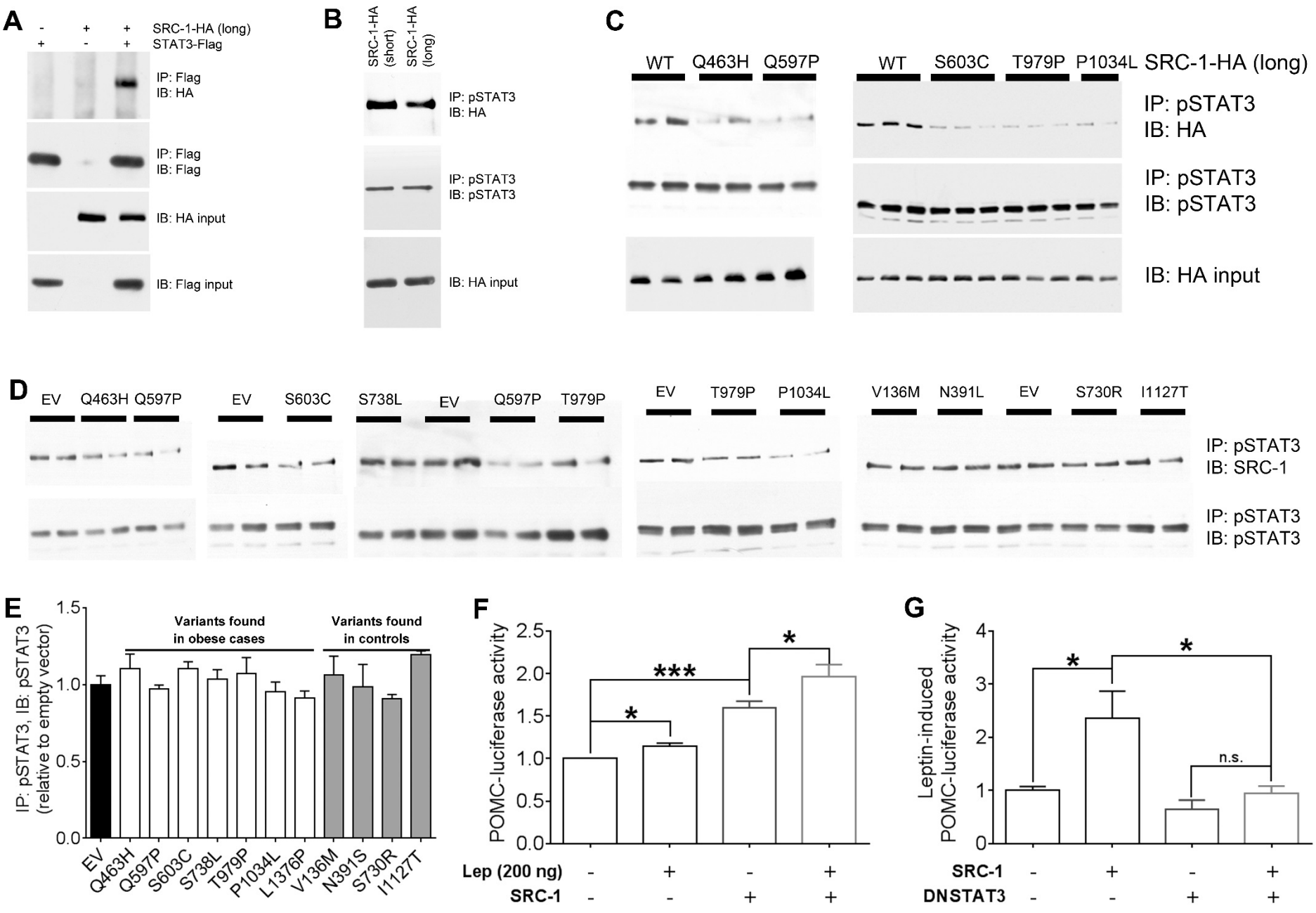
A
SRC-1-HA (long)
STAT3-Flag
IP: Flag
IB: HA
IP: Flag
IB: Flag
IB: HA input
IB: Flag input
B
SRC-1-HA (short)
SRC-1-HA (long)
IP: pSTAT3
IB: HA
IP: pSTAT3
IB: pSTAT3
IB: HA input
C
WT
Q463H
Q597P
WT
S603C
T979P
P1034L
SRC-1-HA (long)
IP: pSTAT3
IB: HA
IP: pSTAT3
IB: pSTAT3
IB: HA input
D
EV
Q463H
Q597P
EV
S603C
S738L
EV
Q597P
T979P
EV
T979P
P1034L
V136M
N391L
EV
S730R
I1127T
IP: pSTAT3
IB: SRC-1
IP: pSTAT3
IB: pSTAT3
E
IP: pSTAT3, IB: pSTAT3
(relative to empty vector)
Variants found in obese cases
Variants found in controls
EV
Q463H
Q597P
S603C
S738L
T979P
P1034L
L1376P
V136M
N391S
S730R
I1127T
F
POMC-luciferase activity
Lep (200 ng)
SRC-1
G
Leptin-induced POMC-luciferase activity
n.s.
SRC-1
DNSTAT3

Figure S4

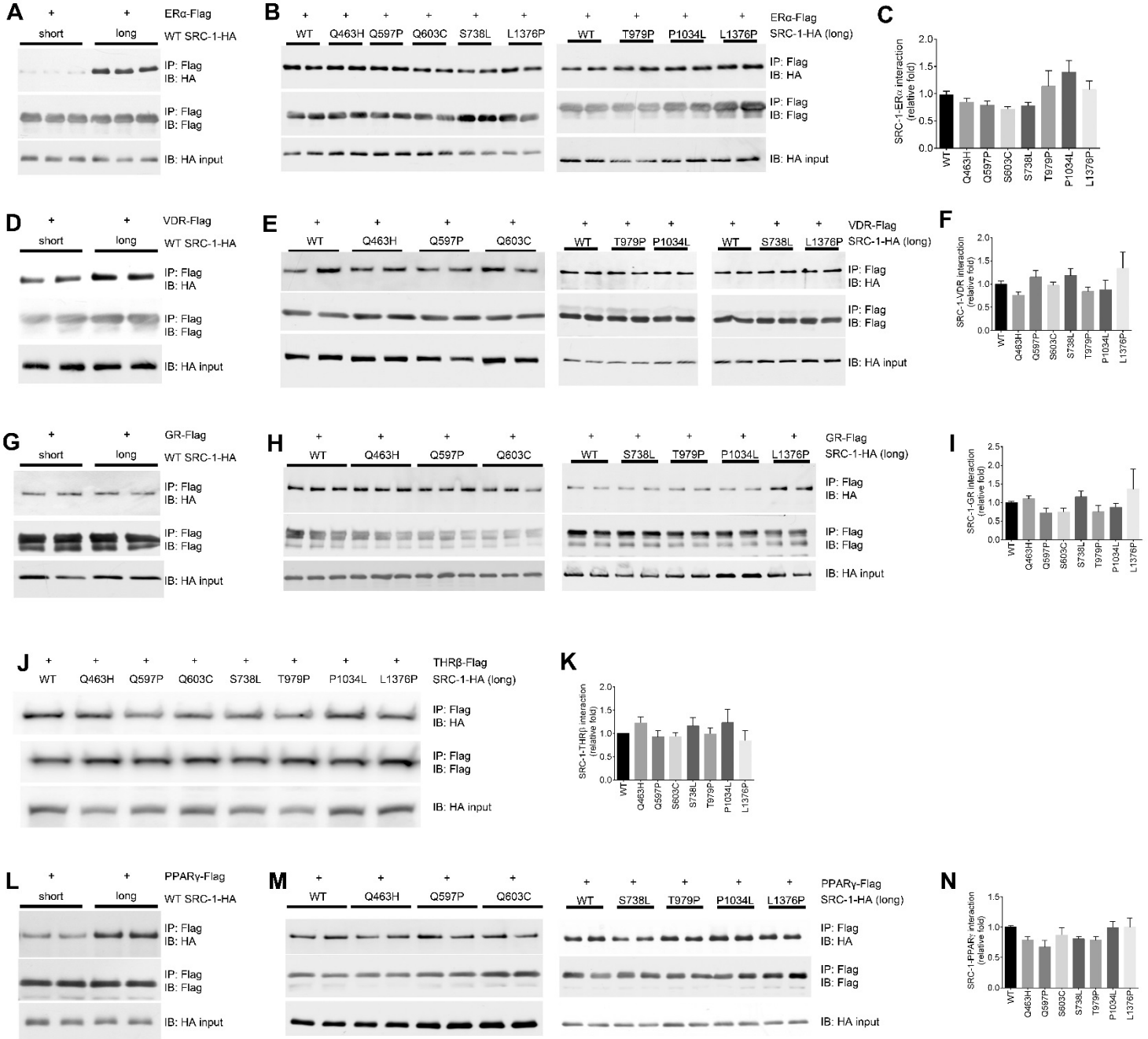
A
ERα-Flag
short
long
WT SRC-1-HA
IP: Flag
IB: HA
IP: Flag
IB: Flag
IB: HA input
B
WT
Q463H
Q597P
Q603C
S738L
L1376P
T979P
P1034L
ERα-Flag
SRC-1-HA (long)
C
SRC-1-ERα interaction (relative fold)
D
VDR-Flag
E
VDR-Flag
F
SRC-1-VDR interaction (relative fold)
G
GR-Flag
H
GR-Flag
I
SRC-1-GR interaction (relative fold)
J
THRβ-Flag
K
SRC-1-THRβ interaction (relative fold)
L
PPARγ-Flag
M
PPARγ-Flag
N
SRC-1-PPARγ interaction (relative fold)

Steroid Receptor Coactivator-1 Modulates the Function of Pomc Neurons and Energy Homeostasis

Yang et al.

Supplementary Figure 1. SRC-1 effects in Pomc neurons.

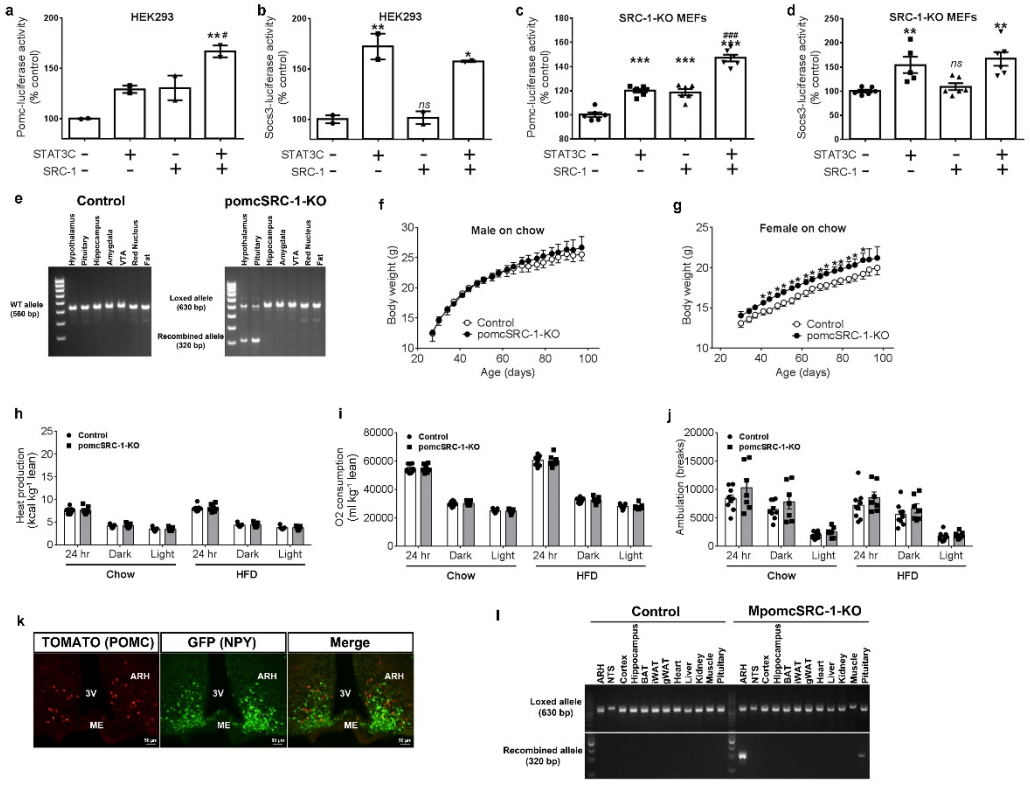

Numbers of mice/experiments are indicated; data are presented as mean ± SEM and compared using T-tests or two-way ANOVA followed by post hoc Sidak tests (#). (A-D) Effects of overexpressed constitutively active STAT3 and SRC-1 on Pomc- or Socs3-luciferase activity in HEK293 cells (a-b) and SRC-1-KO MEF cells (c-d) (n=2-6); * P<0.05, ** P<0.01 and *** P<0.001 vs. empty vectors; # P<0.05 and ### P<0.001 vs. STAT3 alone. (e) Validation of pomcSRC-1-KO mice. PCR amplification of genomic DNA from various brain regions, pituitary and fat. The WT SRC-1 allele (560 bp) was detected in all tissues from a control mouse. The loxed SRC-1 allele (630 bp) was detected in all tissues from a pomcSRC-1-KO mouse, but the recombined SRC-1 allele (320 bp) was only detected in POMC cell-containing tissues (the hypothalamus and pituitary). VTA, ventral tegmental area. (f-g) Body weight of male (f) or female (g) control and pomcSRC-1-KO mice fed regular chow (n=6-13). (h-j) Metabolic phenotypes in male pomcSRC-1-KO mice. 12-week old male control and pomcSRC-1-KO mice with matched body weight, lean mass and fat mass were adapted to the CLAMS chambers. Mice were subjected to a 2-day-chow-2-day-HFD protocol, and chow was replaced by HFD before the onset of dark cycle on day 3. Heat production (h), O2 consumption (i) and ambulatory movement (j) were continuously monitored and averaged for 2-day chow feeding period and for 2-day HFD feeding period (n=7/9). (k) Distribution of TOMATO (induced by *Pomc-CreER*) and GFP (driven by *Npy* promoter) in the ARH of *Pomc-CreER/Rosa26-tdTOMATO/Npy-GFP* mice. No neurons were double labelled, indicating that the mature Pomc neurons targeted by *Pomc-CreER* were segregated from mature Npy neurons. Scale bar=50 µm. 3V, 3rd ventricle; ARH, arcuate nucleus of the hypothalamus; ME, median eminence. (l) PCR amplification of loxed allele and recombined allele in various tissues collected from control vs. Mpomc-SRC-1-KO mice. **Source data are provided as Source Data Fig S1.xlsx.**

Supplementary Figure 2. Leptin-induced effects.

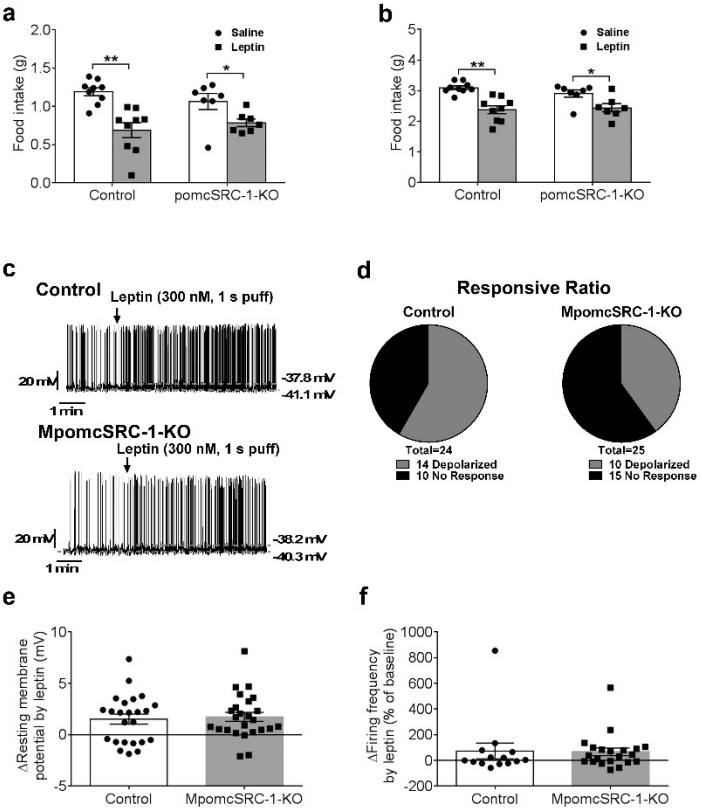

Numbers of mice/neurons are indicated; data are presented as mean ± SEM and compared using T-tests or two-way ANOVA followed by post hoc Sidak tests (#). (a-b) Two-hour fasted mice (12 weeks of age) received i.p. injections of saline/leptin (5 mg/kg) 15 min prior to refeeding and food intake was record for 4 hours (a) or 24 hours (b) afterwards (n=7/9); * P<0.05 and ** P<0.01. (c) Representative traces for leptin-induced depolarization, in the absence of synaptic blockers, in mature Pomc neurons from control mice vs. from MpomcSRC-1-KO mice after one-week HFD feeding. (d) Responsive ratio (depolarization is defined as >2 mV elevations in resting membrane potential, P=0.1994 in $\chi 2$ test). (e-f) Summary quantification of leptin-induced depolarization (e) and increases in firing frequency (f) in two groups (n=14-25). **Source data are provided as Source Data Fig S2.xlsx.**

Supplementary Figure 3. Mutations in SRC-1 impair SRC-1-pSTAT3 interaction.

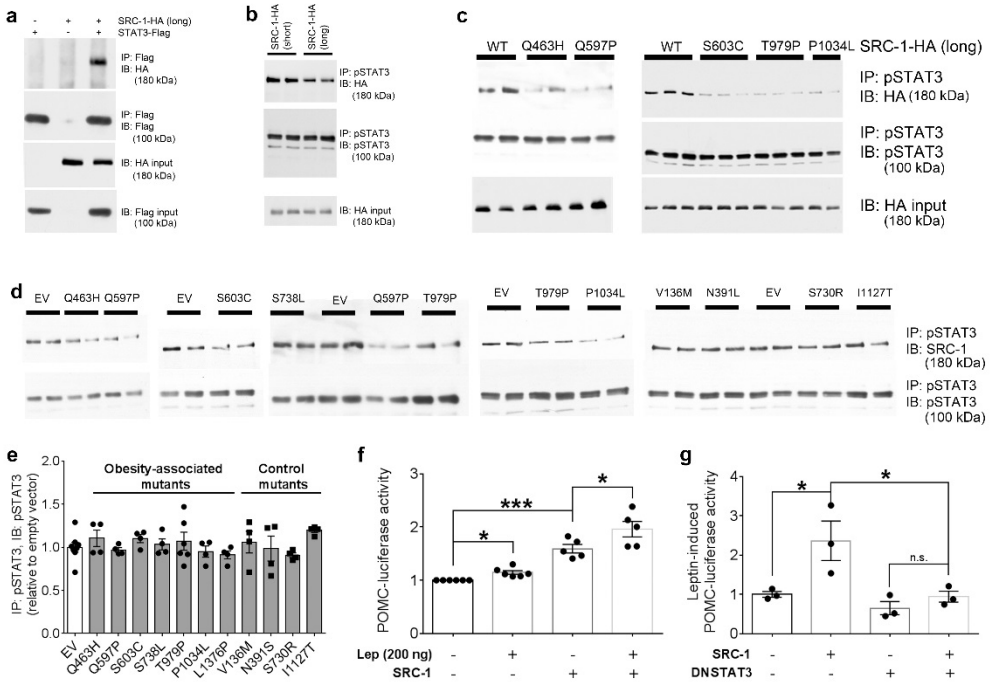

(a) HEK293 cells were transfected with STAT3-Flag alone, WT SRC-1-HA (the long isoform) alone, or the combination of both. Interactions between the STAT3 and SRC-1 were determined by CoIP experiments using anti-Flag and anti-HA antibodies. Representative blots showing interactions between STAT3 and SRC-1, and inputs of HA and Flag. (b) HEK293 cells were transfected with leptin receptor vector and STAT3 vector. Cells were treated with leptin (200 ng/ml, 15 min) to induce phosphorylation of STAT3. pSTAT3 was purified and incubated with long or short isoform of WT SRC-1, and interactions between the pSTAT3 and SRC-1 were determined by CoIP experiments using anti-pSTAT3 and anti-HA antibodies. Representative blots showing interactions between pSTAT3 and SRC-1 and inputs of SRC-1-HA (n=4). (c) HEK293 cells were co-transfected with leptin receptor vector and human STAT3 vector. Cells were treated with leptin (200 ng/ml, 15 min) to induce phosphorylation of STAT3. pSTAT3 was purified and incubated with the long isoform of human SRC-1-HA (WT or obesity-associated mutants), and interactions between the pSTAT3 and SRC-1 were determined by CoIP experiments using anti-pSTAT3 and anti-HA antibodies. (d) HEK293 cells were cotransfected with leptin receptor vector, STAT3 vector, and mutant SRC-1 mutant vector (or empty vector). Cells were treated with leptin (200 ng/ml, 15 min) to induce phosphorylation of STAT3 and interactions between the pSTAT3 and total SRC-1 were determined by CoIP experiments using anti-pSTAT3 and anti-SRC-1 antibodies. (e) Quantification of pSTAT3 inputs (IP: pSTAT3, IB: pSTAT3, n=4-8). (f) Neuro2A cells were co-transfected with leptin receptor vector, a POMC luciferase expression reporter construct, and wild-type human SRC-1 (or empty vector). Cells were stimulated with 200ng/ml leptin or vehicle for 15 minutes and then incubated for 6 hours, following which luminescence was measured (n=5/6). (g) Neuro2A cells were co-transfected with leptin receptor vector, a POMC luciferase expression reporter construct, and wild-type human SRC-1, a dominant negative STAT3 mutant, or their combination. Cells were all stimulated with 200ng/ml leptin for 15 minutes and then incubated for 6 hours, following which luminescence was measured (n=3);* P<0.05 and *** P<0.001 in two-way ANOVA followed by pairwise tests with a Sidak adjustment. Data were presented as mean ± SEM. **Source data are provided as Source Data Fig S3.xlsx.**

Supplementary Figure 4. Interactions between mutant SRC-1 and nuclear receptors.

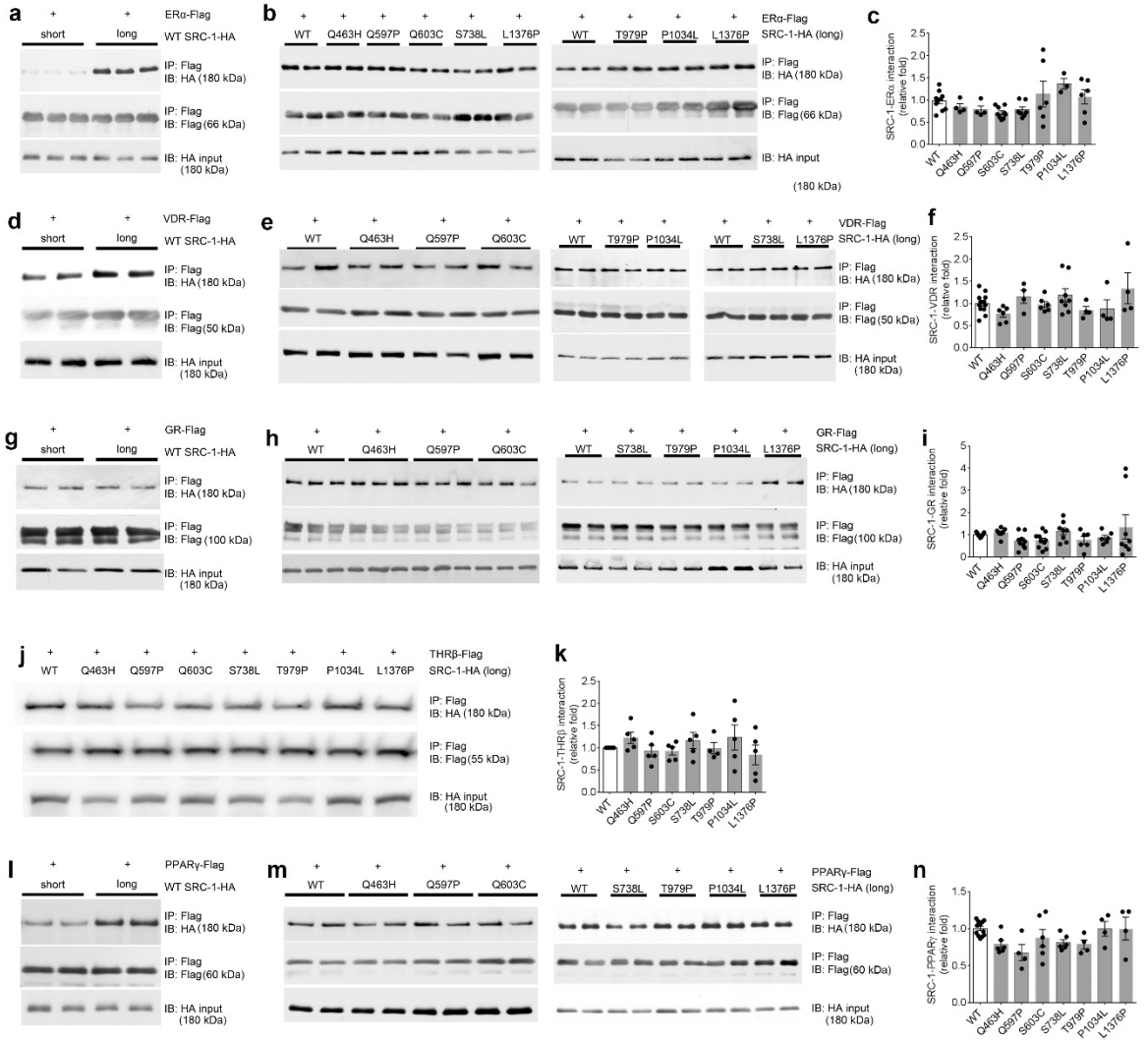

Numbers of experiments are indicated; data are presented as mean ± SEM and compared using one-way ANOVA followed by post hoc Sidak tests. (a) HEK293 cells were transfected with ERα-Flag and treated with 17β-estradiol (0.2 µg/ml, 30 min) to stimulate ERα. ERα was purified and incubated with the short or long isoform WT SRC-1-HA vectors, and interactions between the ERα and SRC-1 were determined by CoIP experiments using anti-Flag and anti-HA antibodies. (b-c) HEK293 cells were transfected with ERα-Flag and were treated with 17β-estradiol (0.2 µg/ml, 30 min) to stimulate ERα. ERα was purified and incubated with the SRC-1 (long isoform WT or one of the 7 mutants), and interactions between the ERα and SRC-1 were determined by CoIP experiments using anti-Flag and anti-HA antibodies. (b) Representative blots showing interactions between ERα and SRC-1 (WT or all 7 mutants), and inputs of ERα and SRC-1-HA. (c) Summary quantification for WT and all 7 SRC-1 mutants. Comparative folds were calculated as the ratios of HA blots and HA inputs (n=3-10). (d) HEK293 cells were transfected with VDR-Flag and treated with 1,25-dihydroxyvitamin D_3 (0.2 µM, 30 min) to stimulate VDR. VDR was purified and incubated with the short or long isoform WT SRC-1, and interactions between the VDR and SRC-1 were determined by CoIP experiments using anti-Flag and anti-HA antibodies. (e-f) HEK293 cells were transfected with VDR-Flag and treated with 1,25-dihydroxyvitamin D_3 (0.2 µM, 30 min) to stimulate VDR. VDR was purified and incubated with SRC-1 (long isoform WT or one of the 7 mutants), and

interactions between the VDR and SRC-1 were determined by CoIP experiments using anti-Flag and anti-HA antibodies. (e) Representative blots showing interactions between VDR and SRC-1 (WT or all 7 mutants), and inputs of VDR and SRC-1-HA. (f) Summary quantification for WT and all 7 SRC-1 mutants (n=4-12). (g) HEK293 cells were transfected with GR-Flag and treated with dexamethasone (10 μM, 30 min) to stimulate GR. GR was purified and incubated with the short or long isoform WT SRC-1, and interactions between the GR and SRC-1 were determined by CoIP experiments using anti-Flag and anti-HA antibodies. (h-i) HEK293 cells were transfected with GR-Flag and treated with dexamethasone (10 μM, 30 min) to stimulate GR. GR was purified and incubated with SRC-1 (long isoform WT or one of the 7 mutants) and interactions between the GR and SRC-1 were determined by CoIP experiments using anti-Flag and anti-HA antibodies. (h) Representative blots showing interactions between GR and SRC-1 (WT or all 7 mutants), and inputs of GR and SRC-1-HA. (i) Summary quantification for WT and all 7 SRC-1 mutants. Comparative folds were calculated as the ratios of HA blots and HA inputs (n=6-10). (j-k) Cell lysate from THRβ-Flag transfected HEK-293 cells were incubated with HA-SRC-1 cell lysate (long isoform WT or one of the 7 mutants) overnight with 1 μM T3 thyroid hormone. Interactions between THRβ and SRC-1 were determined by CoIP experiments using anti-Flag and anti-HA antibodies. (j) Representative blots showing interactions between THRβ and SRC-1 (WT or all 7 mutants), and inputs of THRβ and SRC-1-HA. (k) Summary quantification for WT and all 7 SRC-1 mutants. Comparative folds were calculated as the ratios of HA blots and HA inputs (n=4/5). (l) HEK293 cells were transfected with PPARγ-Flag and treated with rosiglitazone (50 μM, 30 min) to stimulate PPARγ. PPARγ was purified and incubated with the short or long isoforms of WT SRC-1, and interactions between the PPARγ and SRC-1 were determined by CoIP experiments using anti-Flag and anti-HA antibodies. (m-n) HEK293 cells were transfected with PPARγ-Flag and treated with rosiglitazone (50 μM, 30 min) to stimulate PPARγ. PPARγ was purified and incubated with the long isoform of SRC-1 (WT or one of 7 mutants), and interactions between the PPARγ and SRC-1 were determined by CoIP experiments using anti-Flag and anti-HA antibodies. (m) Representative blots showing interactions between PPARγ and SRC-1 (WT or all 7 mutants), and inputs of PPARγ and SRC-1-HA. (n) Summary quantification for WT and all 7 SRC-1 mutants (n=4-12). **Source data are provided as Source Data Fig S4.xlsx.**

126 **Supplementary Table 1. Primer sequences.**

Gene/Protein	Species	Primer Sequence	Primer Names	Accesson#
Cyclophilin	mouse	5`tggagagcaccaagacagaca	CYCLO-QF	M60456
		5`tgccggagtcgacaatgat	CYCLO-QR	
POMC	mouse	5'gaggccactgaacatctttgtc	mPOMC-QF	NM_008895
		5'gcagaggcaaacaagattgg	mPOMC-QR	
SOCS3	mouse	5'cacctggactcctatgagaaagtg	mSOCS3-QF	NM_007707
		5'gagcatcatactgatccaggaact	mSOCS3-QR	
POMC-promoter	mouse	5'gtttgggagcttggtgtgtt	POMC-F1	
Site 1		5'ggtgcctgcctaatctacca	POMC-R1	
POMC-promoter	mouse	5'ttcccatcattggggaaatc	POMC-F2	
Site 2		5'tcttgcagatcggagtggaa	POMC-R2	
POMC-promoter	mouse	5'gagacagaggcccagacatttt	POMC-F3	
Site 3		5'ccgagaatgaaagttgtggtgaa	POMC-R3	

127

128

129 **KEY RESOURCES TABLE**

REAGENT or RESOURCE	SOURCE	IDENTIFIER
Antibodies		
rabbit anti-pSTAT3 antibody	Cell Signaling	9145s
biotinylated anti-rabbit secondary antibody	Vector Labs	BA-1000
rabbit monoclonal SRC-1 (128E7) antibody	Cell Signaling	2191s
monoclonal anti-β-Actin antibody (AC-15)	Sigma	A5441
Peroxidase-AffiniPure Goat Anti-Mouse IgG (H+L)	Jackson ImmunoResearch	115-035-166
Peroxidase-AffiniPure Goat Anti-Rabbit IgG (H+L)	Jackson ImmunoResearch	111-035-144
Stat3 Antibody (C-20)STAT3	Santa Cruz	sc-482
Monoclonal ANTI-FLAG® M2 antibody	Sigma	F3165
Chemicals, Peptides, and Recombinant Proteins		
tamoxifen	sigma	T-5648
leptin	HARBOR-UCLA Research And Education Institute	N/A
17β-estradiol	Sigma	
Vitamin D3 (Calcitriol)	TOCRIS	2551
dexamethasone	Sigma	D4902
rosiglitazone	ADIPOGEN	AG-CR1-3570
Experimental Models: Cell Lines		
SRC-1 KO MEF	This paper	N/A
Experimental Models: Organisms/Strains		
Mouse: Pomc-Cre	Jackson Laboratory	005965
Mouse: Pomc-CreER	Berglund, et al. 2013	N/A
Mouse: SRC-$1^{lox/lox}$	Yamada et al., 2004	N/A
Mouse: Rosa26-tdTOMATO	Jackson Laboratory	007909
Mouse: NPY-GFP	Jackson Laboratory	006417
Mouse: SRC-$1^{L1376P/+}$	This paper	N/A
Mouse: SRC-1-KO	Xu et al., 1998	N/A
Recombinant DNA		
Psg5 SRC-1	Louet, et al., 2010	N/A
pRc/CMV-STAT3; STAT3C-Flag	Horvath, et al., 1995	N/A
pcDNA3.1-LepR	This paper	N/A
pGL3-SOCS3-Luc 6T1	Auernhammer et al., 1999	N/A
pGL3-rPOMC-Luc	Zhang, et al., 2011	N/A
pGL3-hPomc-Luc	This paper	N/A
pcDNA3.1-hSRC-1-HA	This paper	N/A
pcDNA3.1-hSRC-1-Myc	This paper	N/A
pcDNA3.1-hERα-Flag	This paper	N/A
pcDNA3.1-hPPARγ-Flag	This paper	N/A
pcDNA3.1-hGR-Flag	This paper	N/A
pcDNA3.1-hGR-Flag	This paper	N/A
pRL-SV40	Promega	E2231